Heliyon 10 (2024) e37780

Contents lists available at ScienceDirect

Heliyon

journal homepage: www.cell.com/heliyon

Research article

Evaluating the strength characteristics of mixtures of municipal solid waste incineration bottom ash and reddish laterite clay for sustainable construction

Chwen-Huan Wang [a], Li Fang [b,*], Dave Ta-Teh Chang [a], Ching-Jui Hsu [c], Yu-Tang Hu [a]

[a] Dept. of Civil Engineering, Chung Yuan Christian University, No. 200, Zhongbei Rd., Zhongli Dist., Taoyuan City 320314, Taiwan, ROC
[b] School of Civil Engineering, FuJian University of Technology, Fuzhou 350118, China
[c] Long Chin Construction Co.'Ltd, Kaohsiung City 81368, Taiwan, ROC

ARTICLE INFO

Keywords:
Municipal solid waste incineration bottom ash
Reddish laterite clay
Direct shear test
Sustainable construction

ABSTRACT

This study examines effects of mixing municipal solid waste incineration bottom ash (MSWI-BA) with reddish laterite clay (RLC), evaluating factors such as vertical stress, mixing ratio, curing period, and the addition of lime. A total of 153 direct shear tests were conducted to thoroughly assess the mixture's strength characteristics. Vertical stress levels of 85.5 kPa, 172.4 kPa, and 259.3 kPa were used to simulate varying stress conditions, while mixing ratios of 40 %, 80 %, 100 %, and 120 % were applied to explore potential applications of recycled MSWI-BA with clayey soils. A fast-curing approach was employed, with curing periods of 24, 48, and 72 h, to investigate the time-dependent strength development under controlled conditions. A three-way ANOVA analysis confirmed that mixing ratio, curing period, and vertical stress significantly impacted both peak and residual shear strength. The 100 % MSWI-BA mixture, with or without 1 % lime, exhibited optimal performance, providing the pronounced shear strengths and dilative behavior. The study found that MSWI-BA significantly improved shear strength ratios compared to the RLC, with improvement ratios ranging from 1.439 to 2.460 across stress levels. Additionally, upper and lower bound equations for peak and residual strength ratios were developed, providing predictive tools for mixture design. Cohesion values in the range of 8.3–128.9 kPa and friction angles from 40.6° to 44.1° were achieved, surpassing or matching those reported in similar research. The study employed Bolton's (1986) dilatancy model, finding α values between 0.61 and 0.71, comparable to those in studies of granular materials. These results highlight the effectiveness of adding MSWI-BA and lime in enhancing reddish laterite soil stabilization through both chemical and mechanical means, making it a sustainable and cost-effective approach for civil engineering projects by improving material strength, reusing local soils, recycling waste, and reducing carbon footprints.

Abbreviations: CBR(California Bearing Ratio), MSW(Municipal Solid Waste); COV(Coefficient of Variation), MSWI (Municipal Solid Waste Incineration); MSWI-BA(Municipal Solid Waste Incineration Bottom Ash), MSWI-FA(Municipal Solid Waste Incineration Fly Ash); MSWI-BA-RLC ((Municipal Solid Waste Incineration Bottom Ash and Reddish Laterite Clay), RLC(Reddish Laterite Clay); UHI (Urban Heat Island), USCS (Unified Soil Classification System).

* Corresponding author.
E-mail addresses: chwang@cycu.edu.tw (C.-H. Wang), 19902341@fjut.edu.cn (L. Fang), ttateh@cycu.edu.tw (D.T.-T. Chang), zxc860214@gmail.com (C.-J. Hsu), hag75393@gmail.com (Y.-T. Hu).

https://doi.org/10.1016/j.heliyon.2024.e37780
Received 21 June 2024; Received in revised form 9 September 2024; Accepted 10 September 2024
Available online 10 September 2024

1. Introduction

Solid waste, including municipal solid waste (MSW), is managed through various strategies, with waste incineration being a key approach. Municipal solid waste incineration (MSWI) addresses this problem by converting waste into ash, flue gases, heat, and energy, thereby reducing the need for landfills. Taiwan is one of the most densely populated countries in Asia, leading to a substantial amount of waste generation. According to the statistical data from Environmental Protection Administration in Taiwan, the total amount of MSW generated in 2021 was approximately 10.05 million tons. Of this amount, approximately 5.6 million tons were recycled, and 247 thousand tons were disposed in landfills. In 2022, there were in total of 25 waste incineration plants in Taiwan. The total amount of municipal solid waste (MSW) received and incinerated was 6.2 million tons, resulting in 1.1 million tons of residues from the incineration process. Despite these efforts, Taiwan is still facing significant challenges in managing its waste. In recent years, a circular economy has been promoted globally, including in Taiwan, to reduce the consumption of natural resources. Municipal solid waste incineration (MSWI) has emerged as a recycling strategy of interest in civil engineering, owing to its favorable engineering properties. This approach not only helps reduce waste but also contributes to supporting the circular economy. For our research, the focus is on the design purposes of the roadway system by using MSWI waste materials. To fully realize the benefits of incorporating MSWI residues in engineering projects and to support a sustainable circular economy, it is essential to investigate the strength characteristics of mixtures containing MSWI residues. This includes studying properties such as cohesion, friction angle, shear strength, and dilation angles. Understanding these properties will ensure the safe and effective application of MSWI materials in construction, optimizing their performance and contribution to sustainability.

Reusing MSWI residues in the construction industry with local soils aligns with the goals of a sustainable circular economy. The construction industry significantly contributes to CO_2 emissions through the life cycle of buildings [1,2], including material production, transportation, and construction activities. The CO_2 emissions of the construction industries vary globally, with substantial contributions from the production systems in different countries. For example, the construction industries in Russia, India, and China have notably high CO_2 intensities [3]. Transporting raw materials to a concrete plant and then to the construction site can account for approximately 80 % of the embodied energy and CO_2 emissions in concrete production [4]. Emissions from construction sites, including those from fuel-consuming processes and machinery, contribute significantly to the overall carbon footprint [5]. Transport during the construction of new buildings is the largest source of emissions on construction sites [6]. When a building is retired and enters the demolition and rebuild phase, this process significantly contributes to emissions [6].

By replacing these materials with MSWI Bottom Ash (MSWI-BA) and MSWI Fly Ash (MSWI-FA), the carbon emissions from material production are significantly reduced [7,8]. Additionally, utilizing these waste materials helps divert them from landfills [8,9], promoting a circular economy [10,11], thus contributing to overall carbon footprint reduction. Utilizing MSWI residues, including MSWI-BA and MSWI-FA, offer numerous benefits when used in construction projects. These materials are by-products of waste incineration processes, making them readily available and cheaper compared to traditional construction materials [7,12]. The reduction in the need for natural aggregates [13], coupled with decreased transportation costs due to local availability, further contributes to cost savings [14]. This makes MSWI residues an economically attractive option for construction projects [7,9,15].

MSWI residues possess favorable characteristics as granular materials, demonstrating strong structural properties due to their high temperature incineration process. Zekkos et al. (2013) [16] performed soil index tests, including grain size distribution, specific gravity, and surface morphology. Laboratory investigations were conducted such as compaction, shear velocity, direct shear testing, and triaxial testing on MSWI-FA and MSWI-BA. The geotechnical characterizations of these materials indicated that their shear strength can exceed that of sandy soils. Lee et al. (2017) [17] conducted a series of triaxial tests to investigate the mechanical properties of MSWI-BA. The study concluded that the behavior of MSWI-BA was similar to that of dense sands. Huang et al. (2020) [18] conducted a series of laboratory tests, including direct shear tests and California bearing ratio (CBR) tests, with varying water contents and dry densities. Their findings suggested that MSWI-BA can serve as a viable alternative to subgrade materials. Juarez et al. (2023) [19] presented the shear strength parameters of dry MSW post-mechanical sorting, which found strain hardening behavior and varying friction angles and cohesion values. Dehdari et al. (2021) [20] utilized a large direct shear device to test MSW samples, finding friction angles of 31.4° (consolidated-drained tests) and 38.6° (consolidated-undrained tests) with near-zero cohesion.

To evaluate the granular effect of the MSWI-BA, dilatancy behavior is a significant factor to consider when examining the strength behavior. Dilatancy is the tendency of granular soils to expand in volume when subjected to shear stress. Dilatancy affects the strength and stiffness of granular soils and is influenced by factors such as morphology, particle shape, size, density, and moisture content [21–23]. Rowe (1962) [24] presented experiments on random masses of materials and established the relationship between the rate of dilatancy and the maximum stress ratio. Bolton (1986) [25] studied 17 different types of sand, focusing on the friction angle differences between peak and critical state conditions, linking the difference in dense sand to dilatancy during shearing. This research extended to examining dilatancy in cemented sand and clayey soils, beyond just granular materials. Chu et al. (2004) [26] examined the experimental data and confirmed that the stress-dilatancy behavior of sand and clay can be both described by the stress path and strain path. Wang and Leung (2008) [27] found in triaxial tests that increased shearing strain in cemented sand leads to peak strength and bond breakage. During the post-peak strength stage, the shear strength diminished, corresponding with a reduction in material friction, and concentrated along the shearing band at higher strains.

In addition to its granular behavior, the chemical stabilization properties (pozzolanic reaction) of MSWI-BA greatly influences mixture strength. With a high content of calcium oxide (*CaO*), MSWI-BA can neutralize acidity, reduce soil plasticity, and enhance material strength when mixed with clayey soils. MSWI-BA generally contains around 20 %–40 % of *CaO* [13,28–31], with some studies reporting as low as approximately 10 % [13,32] and others as high as approximately 50 % [13,31]. The *CaO* in MSWI-BA reacts with

water to form calcium hydroxide ($Ca(OH)_2$), which reacts with soil particles to form a cementing effect. For example, with high level content of *CaO*, MSWI residues can be used as a partial replacement for cement in concrete mixtures, which can provide sufficient engineering characteristics of construction materials [33–36]. Singh and Kumar (2017) [37] experimented the mixture of cement with MSWI ash in various curing periods. Results indicated that the combinations can be used as a lightweight material with satisfactory strength characteristics. In soil stabilization approaches, it is common to incorporate lime into soils due to its advantage from pozzolanic reaction. Lime, containing components of *CaO* typically contains approximately 50 % (or higher) of *CaO* [28,38], and exhibit pozzolanic properties that react with the soil's silica and alumina components. This reaction produces cementitious compounds and establishes cohesive soil structures. This pozzolanic reaction provided by added lime can effectively enhance the strength characteristics [38–40]. Zang et al. (2020) [41] investigated the effect of temperature and time on the reactivity and strength of lime-soil mixtures. The results showed that unconfined compressive strength significantly increased after 7 days of curing period. Feng et al. (2020) [42] studied how lime and cement treatments enhance sandy lean clay stability in highways, finding improvements in unconfined compression strength, California bearing ratio (CBR), and resilient modulus over untreated soils, influenced by curing periods and additive amounts.

The construction and operation of roadway systems contribute CO_2 emissions and exacerbate the urban heat island effect [43]. The use of materials such as asphalt and concrete in roadways is associated with significant CO_2 emissions during their production and installation [44,45]. Incorporating MSWI residues into pavement systems for roadways and parking projects can effectively balance CO_2 emissions and reduce overall environmental impact. Additionally, using MSWI residues in asphalt and base materials leverages waste reuse, reduces reliance on long-distance transportation, and utilizes local resources, further enhancing sustainability. While considering the environmental benefits, it is necessary to maintain or increase the strength characteristics for engineering purposes. MSWI can serve as an alternative material in roadway construction, offering both granular behavior and chemical stabilization [30, 46–50], which can reduce the amount of virgin soil required for construction projects. Townsend et al. (2020) [51] evaluated using MSWI in commercial aggregates for road construction, revealing improved uniformity and bearing capacity, suggesting MSWI's viability as road-base material. Spreadbury et al. (2021) [52] researched MSWI-BA as a base course, examining thickness and water content in lab and field tests. They assessed performance through resilient modulus and deformation under cyclic loading, finding compaction, thickness, and water content as key performance factors. Shi et al. (2022) [53] conducted research on cement-stabilized MSWI BA in pavement base construction to improve mechanical properties and frost resistance, promoting carbon peaking and carbon neutrality in highway engineering. Joumblat et al. (2022) [54] suggested that using MSWI-FA as a partial or full replacement for fine aggregates and mineral filler in asphalt mixtures improved performance while reduced rutting and fatigue cracking potential. Kyungwon et al. (2023) [55] concluded that using 20 % MSWI-BA and 5 % recycled asphalt shingles in hot mix asphalt improved mechanical performance and sustainability. Gowda et al. (2023) [56] investigated the incorporation of MSWI-BA in rubberized asphalt mixtures to enhance mechanical properties and environmental benefits.

Clayey soils are poorly suited for roadway construction due to their susceptibility to volume changes, leading to instability and frequent maintenance. Additionally, their low shear strength, plasticity, and poor workability complicate construction processes and increase costs [57,58]. When using local clayey materials, constructing transportation systems with clay can be problematic due to its high water absorption, causing instability and potential damage. MSWI residues with local clayey soils in construction projects supports the goals of a sustainable circular economy [59–61]. This approach not only reduces the dependency on natural raw materials but also diverts waste from landfills, effectively managing waste and conserving natural resources. By using locally available soils combined with MSWI-BA or MSWI-FA, the transportation emissions and costs associated with long-distance material transport are significantly minimized [62]. The incorporation of MSWI residues with local soils in construction projects can substantially lower the carbon footprint associated with roadway construction [53,63]. Furthermore, MSWI residues can enhance the mechanical properties of construction materials, making them suitable for enhancing the strength of materials [64–66]. The addition of MSWI residues to local clayey soils enhances the characteristics of mixtures and benefits the overall performance of the civil engineering projects [67–71]. The enhanced mechanical properties of the resulting materials contribute to the durability and longevity of construction projects. Huang et al. (2021) [72] performed unconfined compression tests on MSWI-BA and RLC (MSWI-BA-RLC) mixtures, studying the impact of mixing ratio, curing time, and grain size on their mechanical and chemical properties. Results showed that adding MSWI-BA notably increases mixture strength, with higher MSWI-BA ratios transforming the material from clayey to granular. Sun and Sun and Yi (2022) [73] investigated the use of marine clay and MSWI-BA mixtures as fill materials for transportation construction. They found that these mixtures transformed into semi-solid or solid granular materials with improved unconfined compression strength. Zimar et al. (2022) [74] examined the incorporation of MSWI-FA into expansive clay for road pavement, finding that it mitigated swelling and shrinkage issues while improving compressive strength and CBR. Qiu et al. (2023) [75] developed a multi-source solid-waste-based soft soil solidification material, achieving significant increases in unconfined compressive strength for sandy soil, silty clay, and organic clay. The study found the optimal solidifying agent content to be 17 %, yielding compressive strengths of 3.16 MPa, 2.05 MPa, and 1.04 MPa, respectively.

In Taoyuan City, Taiwan, high water content in soil posed construction challenges. Stabilizing clay with lime or concrete reduces plasticity but increases costs and carbon footprint, while using granular materials like sand or gravel has better strength but similar drawbacks. To address this, the authors' team mixed local RLC with MSWI-BA in previous construction projects, achieving compaction and sustainability in pavement subbases while reducing costs and environmental impact. This method enhanced workability and resource efficiency, aligning with sustainable construction practices. To encourage the further utilization of MSWI-BA-RLC, engineers would need the strength parameters associated with the most favorable mixing ratio for their designs. This study aimed to examine the performance of MSWI-BA-RLC mixture based on previous successful field performance experiences. By exploring various factors that could affect the mixture's performance, the findings aimed to contribute the design process and to improve construction experience.

The knowledge gained from this study could be applied to future projects, promoting the use of this mixture in a wider range of construction applications. To assess the impact of MSWI-BA addition on strength parameters for design purposes, this study conducted direct shear tests to evaluate peak and residual shear strength, peak and residual shear strength ratios, cohesion, friction angle, and dilatancy behavior of the mixture.

2. Methodology

2.1. Materials

The Taoyuan platform in northern Taiwan features gently sloping hills and plains with sedimentary rocks. Its top layer, rich in iron and aluminum oxides, is composed of RLC, varying in depth up to 10 m and overlaying a mix of laterite and boulders. The area's groundwater table depth ranges widely due to topographical and climatic factors. This study uses reddish laterite from near Chung Yuan Christian University as a base material to mix with MSWI-BA.

MSWI-BA was collected from a waste incineration plant located within Taoyuan City. The MSWI-BA, primarily derived from household waste, underwent a pre-scanning process to remove larger objects and metal. Field Emission Scanning Electron Microscope (FE-SEM) analysis revealed the MSWI-BA particles had an angular shape (Fig. 1(a)), providing excellent interlocking mechanics for improved shear resistance. The particles also had a flaky and uneven surface (Fig. 1(b)), allowing for effective water absorption and dissipation. When exposed to sunlight, the MSWI-BA quickly dried out, which was advantageous for reducing the water content of the mixture and absorbing water from the surrounding clay.

Table 1 and Fig. 2 show the soil properties and grain size distribution for the materials used in this study. According to the Unified Soil Classification System (USCS), RLC and MSWI-BA are classified as *CH* and *SW*, respectively. Table 2 presents a summary of the chemical composition obtained from the two sample batches collected for this study. The analysis revealed that the values *CaO* content in the samples were 23.73 % and 22.85 %.

2.2. Development of procedure for this study

This article comprises four major sections focused on exploring how MSWI-BA affects the engineering strength properties when combined with RLC. Fig. 3 outlines the study's content flow, with each major step detailed in the following sections.

2.2.1. Mixture design

In this study, the mixture design was based on the moist weight of the materials, taking into account the practical conditions experienced during construction. To evaluate the influence of adding MSWI-BA, different weight percentages were considered in the mixture design. These percentages included 40 %, 80 %, 100 %, and 120 % of MSWI-BA mixed with 100 % of RLC in moist weight. By varying the proportion of MSWI-BA, the study aimed to observe the corresponding changes in the mixture's behavior and performance, allowing for a comprehensive analysis of both the chemical and mechanical effects induced by the incorporation of MSWI-BA.

Adding lime to soil with high water content is a common practice in construction for soil stabilization purposes. However, this can lead to increased construction costs and a higher carbon footprint. To enhance the workability and strength characteristics essential for optimal field performance, this study examined the effects of adding a minimum of 1 % lime (by moist weight) to a MSWI-BA-RLC mixture. The primary objective of this investigation was to comprehensively understand the impact of this minimal lime addition on the strength characteristics of the mixture. This modest 1 % lime addition aimed to provide a practical and effective solution to the challenges posed by excessive water content, while simultaneously promoting the efficient and sustainable use of MSWI-BA as a

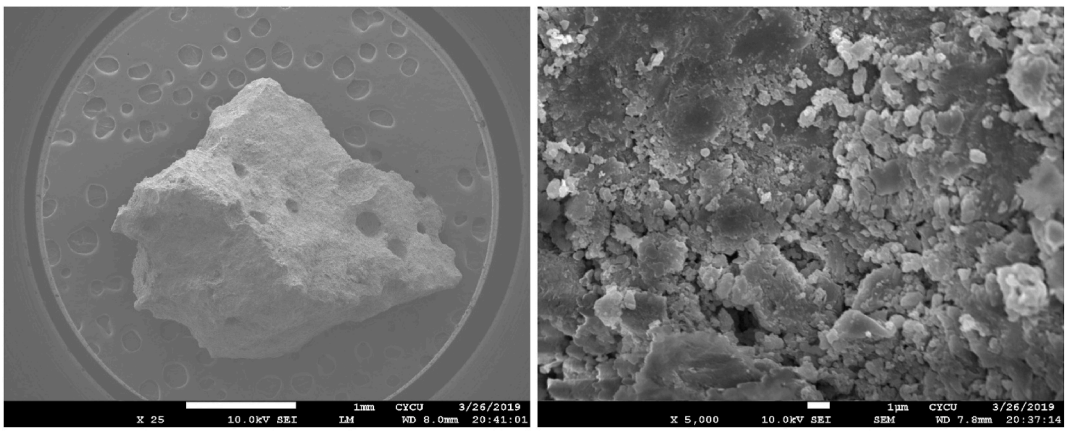

Fig. 1. Particle and surface of the MSWI-BA, magnified (a) 25 times and (b) 5000 times using FE-SEM.

Table 1
Index properties of RLC and MSWI-BA.

Test Item	RLC	MSWI-BA
Specific gravity (G_s)	2.75	2.46
Liquid limit (*LL*)	59–60	–
Plastic limit (*PL*)	20–23	–
Plasticity index (*PI*)	37–40	–
Uniformity coefficient (C_u)	–	8.9–10.0
Coefficient of gradation (C_c)	–	0.8–2.1
Natural water content (*w*)	13.8%-	20.2 %

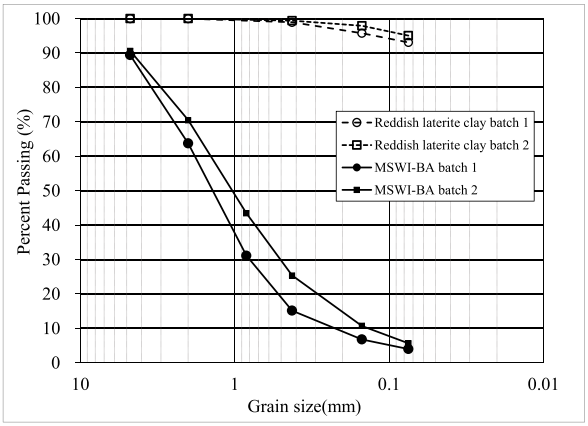

Fig. 2. Grain size distribution of RLC and MSWI-BA.

Table 2
Chemical composition of MSWI-BA in this study.

Chemical Composition	Batch 1 content in %	Batch 2 content in %
Silicon dioxide (SiO_2)	29.24	30.25
Aluminum oxide (Al_2O_3)	6.82	7.14
Sodium oxide (Na_2O)	3.36	3.33
Potassium oxide (K_2O)	1.15	1.1
Magnesium oxide (MgO)	1.9	1.96
Calcium oxide (CaO)	23.73	22.85
Titanium oxide (TiO_2)	1.12	1.15
Ferric oxide (Fe_2O_3)	7.58	8.02
Sulfur trioxide (SO_3)	2.62	2.43
Phosphorus pentoxide (P_2O_5)	5.54	5.11
Manganic oxide (Mn_2O_3)	0.33	0.21
Chlorine (Cl)	2.44	2.46
Loss on ignition	N/A	N/A

valuable construction resource. A comparison was made between mixtures with and without the addition of lime to assess any enhancements or alterations in the strength performance.

2.2.2. Sample preparation

The sample preparation procedure for mixing MSWI-BA with RLC followed a systematic approach to ensure the representative nature of the samples. In civil engineering projects, achieving a sufficient level of compaction was crucial to ensure the stability and durability of the constructed sub-base. The Modified Proctor test based on ASTM D1557 was adopted to provide guidance on achieving the desired relative compaction. In this study, the target relative compaction was determined as 90 %. However, to account for any construction errors or inconsistencies, a higher relative compaction value of 92 % was adopted to all the sample preparation processes.

After compaction, the samples were extracted and prepared for further testing. They were placed in the designated curing conditions, allowing for the pozzolanic reactions to occur and for further development of the mixture's strength properties. To accelerate the curing process and simulate the effects of long-term curing at normal temperature conditions, a fast-curing approach was adopted. This approach involved subjecting the samples to an elevated temperature and high humidity condition for a shorter duration. Terrel et al. (1979) [76] and Transportation Research Board [38] advocated an approach for testing the strength characteristics of lime-soil

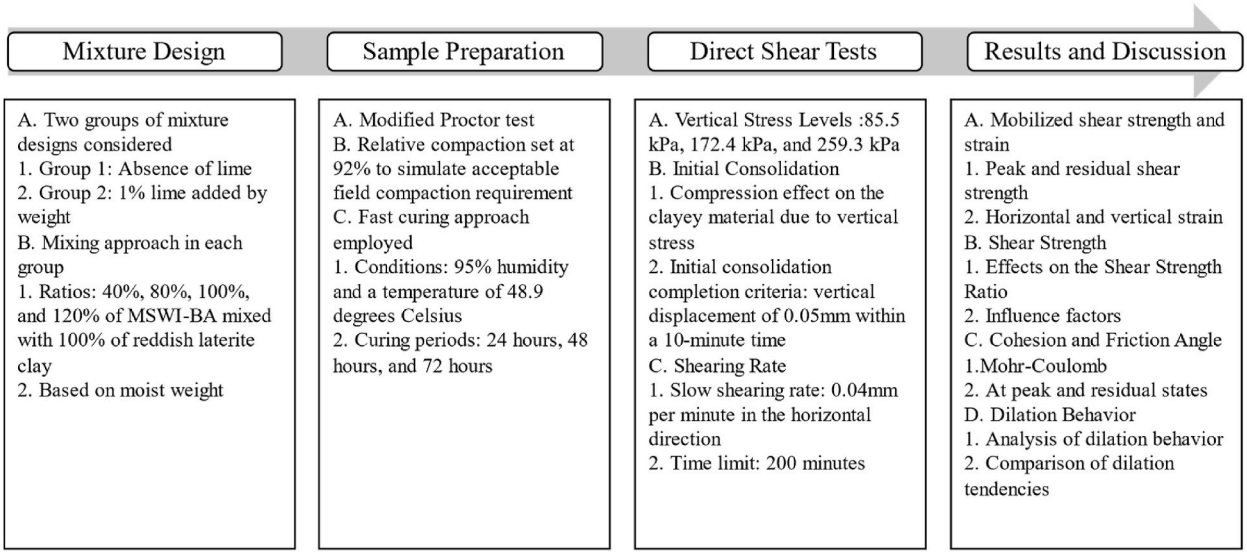

Fig. 3. Components of this article.

stabilization. The lime-soil specimens were placed in a sealed chamber for a duration of 48 h. This chamber sustained a curing environment with 95 % humidity and a temperature of 48.9 °C (120 °F). The choice of 48 h was based on the premise that this accelerated curing period could simulate the strength development and chemical reactions equivalent to 30 days at 21.1 °C (70 °F). In addition to adopting this approach in this study by using the 48-h curing period, two other curing periods of 24 h and 72 h were chosen to examine the effect of different curing durations on the properties of the mixture.

2.2.3. Direct shear tests

The direct shear test was utilized in this study to investigate the shear strength properties of soils. Following the standards of ASTM D3080, soil samples were subjected to a controlled horizontal shearing displacement rate to evaluate their strength behavior. By applying different levels of vertical stress values, data were collected to determine the peak and residual shear strength behaviors. The peak shear strength corresponded to the maximum resistance offered by the soil to resist shearing deformation. The residual shear strength represented the soil's shearing resistance at a large horizontal strain condition. By examining the data at the peak and residual conditions, under various vertical stress testing results, cohesion and friction values were estimated to formulate the Mohr-Coulomb failure criteria. In addition to stress-strength relationships, the direct shear test provided insights into the soil's dilation behavior.

To simulate possible applications of the usage of MSWI-BA mixed with RLC, the designated vertical stress levels included 85.5 kPa, 172.4 kPa, and 259.3 kPa. These values were designed to represent low, intermediate, and high stress conditions, respectively. These simulated stress conditions replicate potential applications in pavement sub-grade systems and a range of ground improvement scenarios.

When a mixture was subjected to vertical stress, the materials could experience both elastic and consolidation settlement. While elastic settlement could occur within a short period, the initial consolidation process might require sufficient time for the clayey materials within the mixture to reach a stable condition. To confirm that the specimen had reached a stable condition and to terminate this initial consolidation process, the termination criterion was defined as a vertical displacement of 0.05 mm within a 10-min time. Once the initial condition was deemed complete, the shearing process began. In the case of mixtures containing both clayey and granular materials, a slow shear rate was selected to capture the shearing behavior of the mixture. A shear rate of 0.04 mm per minute in the horizontal direction was employed in this study. The entire shearing process typically lasted for approximately 200 min, or approximately minimum 10 % of the horizontal shear strain reached.

2.2.4. Number of testing samples

Several factors were considered in this study, including the curing periods, mixing ratios MSWI-BA-RLC mixture, vertical stress levels, and the presence or absence of 1 % lime in the mixtures. The test program was divided into two main groups. Group 1 consisted of tests with MSWI-BA and 0 % lime added, while Group 2 included tests with MSWI-BA and with 1 % lime added. Within each group, different weight ratios were tested, specifically 40 %, 80 %, 100 %, and 120 %. For Group 1, each weight ratio had 2 test sets, and within each test set, tests were conducted under 3 different initial vertical stresses: 85.5 kPa, 172.4 kPa, and 259.3 kPa. Additionally, for each test set in Group 1, 3 curing times were considered: 24 h, 48 h, and 72 h. However, for the 40 % weight ratio, only a curing time of 48 h was used. Group 2 followed a similar structure but included 3 test sets for each weight ratio, except for the 40 % weight ratio, which had only 2 test sets. Like Group 1, each test set in Group 2 was subjected to 3 initial vertical stresses. The curing times for Group 2 were also 24 h, 48 h, and 72 h, except for the 40 % weight ratio, which used only a 48-h curing time. Additionally, for the RLC, 2 test sets were conducted for 3 different initial vertical stresses. As indicating in Table 3, a total of 153 direct shear tests were conducted in this study.

3. Results and discussion

3.1. Peak and residual shear strength

According to the 153 direct shear test results conducted in this study, Tables 4 and 5 present the average peak and residual shear strength values. Each averaged value represents the mean shear strength derived from 2 or 3 test sets in each vertical stress and curing period conditions. To investigate the influence of mixing ratio, curing period, and vertical stress on the average peak and residual shear strength, a three-way ANOVA analysis was conducted to assess their statistical significance. As shown in Table 6, with a p-value threshold of less than 0.05 indicating statistical significance, the factors of mixing ratio, curing period, and vertical stress in both Group 1 and Group 2 exhibit the significant effect on results of average peak and residual shear strength. Conversely, the interactions between mixing ratio and curing period, mixing ratio and vertical stress, and vertical stress and curing time were less significant, suggesting that these three factors produced independent effect to each other.

3.2. Behaviors of mobilized shear strength and strain

This section presents the results and analysis of the influence of various mixing ratios and the presence of lime on the behavior of the MSWI-BA-RLC mixtures. To provide illustrative examples from the overall results, Fig. 4 (results with absence of lime) and Fig. 5 (results with 1 % lime added) illustrate the testing data for various mixing ratios, considering curing period of 48 h and the vertical stress of 172.4 kPa. The figures demonstrate the mobilization of shear strength with increasing horizontal strain, accompanied by the corresponding vertical strain values. For each mixing ratio, 2 testing specimens were conducted as shown in Fig. 4, while 3 testing specimens were conducted as depicted in Fig. 5. For comparison purposes, the results of the RLC, without any MSWI-BA or lime added, are illustrated in Figs. 4 and 5 as 0 % Test 1 and 0 % Test 2.

In this study, the horizontal strain is defined as the ratio of the horizontal displacement to the dimension along the shearing direction, which corresponds to the diameter of the direct shear specimen. The vertical strain is defined as the ratio of the vertical displacement to the initial height of the specimen before applying horizontal force. The initial height for the shearing process should consider any settlement that occurred during the initial consolidation process. To account for this settlement, the initial height of the specimen for the shearing process is determined as the height measured at the completion of the initial consolidation stage.

Fig. 4(a) showed that the RLC without lime had no distinct peak shear strength, with an average residual strength of 79.3 kPa at 172.4 kPa vertical stress. Shear strength increased with higher MSWI-BA mixing ratios: peak strengths rose from 164.929 kPa (40 % ratio) to 229.584 kPa (80 % ratio), and residual strengths from 159.509 kPa to 189.320 kPa. At 100 % and 120 % ratios, peak strengths increased more modestly, from 251.953 kPa to 276.560 kPa, and residual strengths remained similar at 169.315 kPa and 162.304 kPa. This suggests a plateau in strength improvement beyond a 100 % mixing ratio, indicating that further increases in MSWI-BA may not significantly enhance strength.

In the demonstration of the vertical strain versus horizontal strain behavior, Fig. 4(b) showed that the RLC had noticeable contraction behavior. Without lime, increasing the mixing ratio to 40 % led to initial compression transitioning into slight dilation. At 80 % and 100 % ratios, specimens showed dilative behavior, which lessened when the ratio reached 120 %. Specifically, at 12 % horizontal strain, vertical strains were 0.4 %, 2.3 %, 4.3 %, and 3.5 % for 40 %, 80 %, 100 %, and 120 % mixing ratios, respectively. This suggests that the 100 % mixing ratio achieved the maximum dilative behavior, influenced by both chemical and mechanical effects of MSWI-BA addition.

Fig. 5(a) explores shear strength behavior with increased shear strain in mixtures with 1 % lime. Increasing the mixing ratio from 40 % to 120 % shows little difference in shear strength mobilization. Peak shear strengths for 40 %, 80 %, 100 %, and 120 % ratios fluctuates around 334.891 kPa, 307.911 kPa, 280.110 kPa, and 291.142 kPa, respectively. Residual strengths also vary, with averages of 176.931 kPa, 190.997 kPa, 167.478 kPa, and 180.031 kPa for these ratios. Generally, 1 % lime mixtures had higher peak and residual strengths than those without lime, indicating significant impact of 1 % lime addition on shear strength mobilization for different ratios in this study.

Fig. 5(b) shows the vertical versus horizontal strain behavior in 1 % lime-added mixtures. All mixing ratios displayed noticeable dilative behavior, with no significant differences in dilation extent. However, variations were observed, such as larger dilation in test 1 of the 40 % ratio and test 2 of the 100 % ratio. The mixtures, due to the cementation effect of MSWI-BA and lime, showed fragmented

Table 3
Test program in this study.

Mixing ratios	Group1: 0 % Lime			Group 2: 1 % Lime		
	24 Hours	48 Hours	72 Hours	24 Hours	48 Hours	72 Hours
40 %	–	6	–	–	6	–
80 %	6	6	6	9	9	9
100 %	6	6	6	9	9	9
120 %	6	6	6	9	9	9
0 %	6					

"6" represents 2 test sets with 3 vertical stress levels.
"9" represents 3 test sets with 3 vertical stress levels.

Table 4
Results of shear strength for Group1 (0 % lime added) test program.

Group 1: 0 % Lime		Average peak shear strength ratio			Average residual shear strength ratio		
Mixing Ratio	Vertical Stress (kPa)	24 h	48 h	72 h	24 h	48 h	72 h
40 %	85.5	–	113.437	–	–	93.305	–
	172.4	–	164.929	–	–	159.509	–
	259.3	–	228.810	–	–	224.551	–
80 %	85.5	132.220	158.735	131.486	91.819	93.305	90.350
	172.4	180.700	229.584	192.821	147.278	189.320	146.177
	259.3	248.279	280.302	247.545	196.493	246.619	210.083
100 %	85.5	152.153	158.297	151.766	94.467	81.536	93.692
	172.4	215.259	251.953	230.746	167.639	169.315	163.380
	259.3	271.784	291.986	308.177	219.518	240.200	230.746
120 %	85.5	142.871	175.926	150.951	83.005	95.492	85.943
	172.4	221.835	276.560	234.323	156.093	162.704	162.337
	259.3	278.029	317.695	301.902	217.428	276.560	233.221

Table 5
Results of shear strength for Group 2 (1 % lime added) test program.

Group 2: 1 % Lime		Average peak shear strength ratio			Average residual shear strength ratio		
Mixing Ratio	Vertical Stress (kPa)	24 h	48 h	72 h	24 h	48 h	72 h
40 %	85.5	–	209.839	–	–	117.309	–
	172.4	–	334.891	–	–	176.931	–
	259.3	–	372.445	–	–	282.625	–
80 %	85.5	188.933	202.870	232.119	88.788	99.370	80.801
	172.4	284.948	307.919	306.064	178.608	190.997	167.968
	259.3	356.443	345.602	376.826	250.620	272.300	226.488
100 %	85.5	192.698	219.142	235.302	97.206	95.492	85.208
	172.4	259.787	280.110	311.451	159.130	167.478	161.847
	259.3	337.160	346.220	380.989	236.526	227.712	243.627
120 %	85.5	173.704	219.647	217.918	89.304	91.369	83.494
	172.4	269.719	291.142	301.412	168.542	180.931	172.865
	259.3	340.698	375.542	387.355	255.782	266.106	216.204

Table 6
Three-way ANOVA analysis p-value results.

Three-way ANOVA p-values	Group 1: 0 % Lime		Group 2: 1 % Lime	
	Average peak shear strength	Average residual shear strength	Average peak shear strength	Average residual shear strength
Mixing ratio	0.001	0.0008	0.001	0.0006
Vertical stress	0.014	0.021	0.013	0.015
Curing period	0.011	0.012	0.01	0.011
Mixing ratio vs. vertical stress	0.093	0.113	0.092	0.102
Mixing ratio vs. curing period	0.115	0.140	0.113	0.12
Vertical stress vs. curing time	0.165	0.183	0.161	0.182

materials (~1 mm–2 mm in size) along the shear plane, indicating fragmentation under shearing forces. This fragmentation is believed to contribute to the observed dilation behavior during testing.

For the sustainable design and construction purposes, mixing approaches aim to maximize the use of local clayey soils with MSWI-BA. However, higher mixing ratios, implying less on-site clay, may not be practical and economical for real-world engineering applications. In this study, the influence of various mixing ratios of MSWI-BA-RLC mixture, with and without 1 % lime, was analyzed to assess their effects on shear strength and strain behavior. The results indicated that a 100 % mixing ratio of MSWI-BA, both with and without the addition of 1 % lime, provides the best performance in terms of shear strength and dilative behavior. Without lime, the 100 % mixing ratio demonstrated the highest peak and residual strengths, as well as maximum dilative behavior, compared to lower or higher mixing ratios. This suggests that the 100 % ratio strikes an optimal balance between the mechanical and chemical contributions of MSWI-BA, enhancing both peak and residual strengths. When 1 % lime was added, the 100 % mixing ratio continued to show favorable performance, although peak and residual strengths were generally higher across all ratios compared to mixtures without lime. The lime addition contributed to increased shear strength and improved the material's behavior under strain, confirming the effectiveness of this combination.

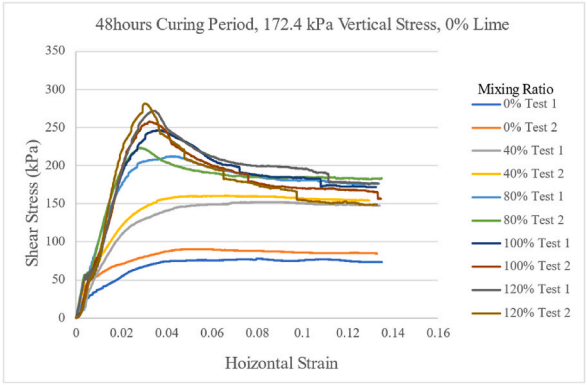

(a)

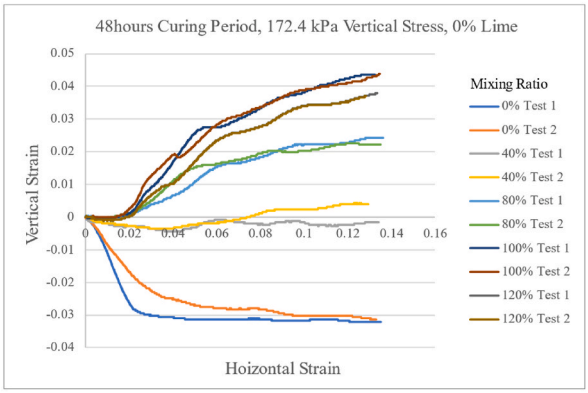

(b)

Fig. 4. Selected results from test group of 0 % lime added: (a) horizontal strain versus shear stress mobilized and (b) horizontal strain versus vertical strain.

3.3. Behaviors of shear strength ratio

The peak and residual shear strength values were averaged based on 2 (for Group1 with 0 % lime added) or 3 (for Group 2 with 1 % lime added) specimens tested for each vertical stress level. For the RLC, since no apparent peak shear strength was observed, only residual shear strength values were averaged from 2 specimens at each vertical stress level. These averaged values were then used to determine the shear strength ratio, calculated by dividing the shear strength value by the corresponding vertical stress value. The results of these calculations are presented in Table 7, Tables 8, and Table 9, representing the testing groups with RLC, Group 1 and Group 2, respectively.

Comparing the Group 1 and 2, Group 2 with 1 % lime generally exhibited higher peak and residual shear strength ratios compared to Group 1 with 0 % lime. For example, at a mixing ratio of 80 %, the peak shear strength ratio for Group 2 was 2.210 at 24 h, while for Group 1 it was 1.546. This suggested that the addition of lime had a positive effect and enhanced the shear strength of the mixtures. When lime is combined with fine-grained soils, the introduction of lime to fine-grained materials can quickly exhibit cation exchange and flocculation-agglomeration reactions in the existence of water [38]. The increased strength ratios observed in Group 2 could be attributed to the effect provided by lime, which improved the interlocking and bonding among mixture materials.

By examining the influence of mixing ratios, the data showed that higher mixing ratios resulted in improved shear strength ratios for both groups. As the mixing ratio increased from 40 % to 120 %, there was a general trend of increasing peak and residual shear strength ratios. For instance, at a stress level of 85.5 kPa and a curing period of 48 h, the peak shear strength ratio increased from 1.327 for a mixing ratio of 40 % to 2.058 for a mixing ratio of 120 % in Group 1. Similarly, the residual shear strength ratio increased from 1.091 to 1.117 for the same mixing ratios and curing period. This indicated that a higher proportion of MSWI-BA in the mixture contributed to enhanced shear strength.

Furthermore, the stress levels exerted on the specimens had a significant influence on the shear strength ratios. Higher stress levels resulted in lower peak and residual shear strength ratios across different mixing ratios and curing times. For example, at a mixing ratio of 100 % and a curing period of 72 h, the peak shear strength ratio for Group 1 at a stress level of 259.3 kPa was 1.188, while for a stress level of 85.5 kPa, it was 1.775.

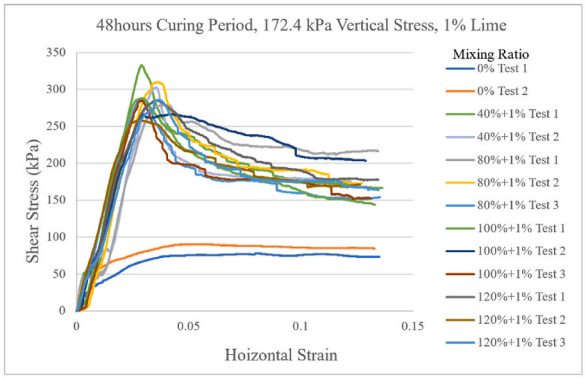

(a)

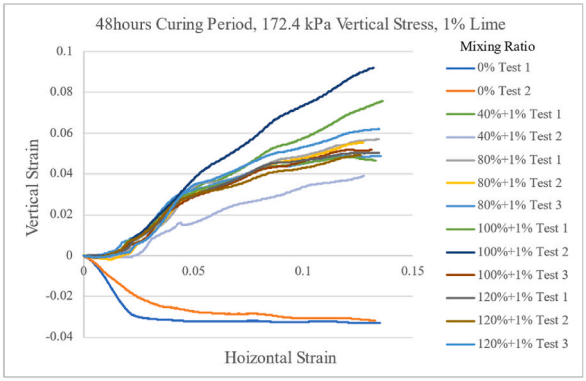

(b)

Fig. 5. Selected results from test group of 1 % lime added: (a) horizontal strain versus shear stress mobilized and (b) horizontal strain versus vertical strain.

Table 7
Results of shear strength ratio for the RLC.

Vertical Stress (kPa)	85.5	172.4	259.3
Shear strength ratio	0.739	0.460	0.411

Table 8
Results of shear strength ratio for Group1 (0 % lime added) test program.

Group 1: 0 % Lime		Peak shear strength ratio			Residual shear strength ratio		
Mixing Ratio	Vertical Stress (kPa)	24 h	48 h	72 h	24 h	48 h	72 h
40 %	85.5	–	1.327	–	–	1.091	–
	172.4	–	0.957	–	–	0.925	–
	259.3	–	0.882	–	–	0.866	–
80 %	85.5	1.546	1.857	1.538	1.074	1.091	1.057
	172.4	1.048	1.332	1.118	0.854	1.098	0.848
	259.3	0.957	1.081	0.955	0.758	0.951	0.810
100 %	85.5	1.780	1.851	1.775	1.105	0.954	1.096
	172.4	1.249	1.461	1.338	0.972	0.982	0.948
	259.3	1.048	1.126	1.188	0.847	0.926	0.890
120 %	85.5	1.671	2.058	1.766	0.971	1.117	1.005
	172.4	1.287	1.604	1.359	0.905	0.944	0.942
	259.3	1.072	1.225	1.164	0.839	1.067	0.899

Table 9
Results of shear strength ratio for Group 2 (1 % lime added) test program.

Group 2: 1 % Lime		Peak shear strength ratio			Residual shear strength ratio		
Mixing Ratio	Vertical Stress (kPa)	24 h	48 h	72 h	24 h	48 h	72 h
40 %	85.5	–	2.454	–	–	1.372	–
	172.4	–	1.943	–	–	1.026	–
	259.3	–	1.436	–	–	1.090	–
80 %	85.5	2.210	2.373	2.715	1.038	1.162	0.945
	172.4	1.653	1.786	1.775	1.036	1.108	0.974
	259.3	1.375	1.333	1.453	0.967	1.050	0.873
100 %	85.5	2.254	2.563	2.752	1.137	1.117	0.997
	172.4	1.507	1.625	1.807	0.923	0.971	0.939
	259.3	1.300	1.335	1.469	0.912	0.878	0.940
120 %	85.5	2.032	2.569	2.549	1.044	1.069	0.977
	172.4	1.564	1.689	1.748	0.978	1.049	1.003
	259.3	1.314	1.448	1.494	0.986	1.026	0.834

The results revealed that curing period affects the shear strength ratios of both Group 1 and Group 2. Comparisons across 24-h, 48-h, and 72-h curing times showed variations in peak and residual shear strengths, with extended curing enhancing pozzolanic reactions and strength. However, the impact of curing time may plateau or decrease after a certain period. For example, Group 1's peak shear strength ratio increased from 24 to 48 h but slightly declined at 72 h. Conversely, Group 2's peak shear strength consistently rose from 24 to 72 h.

Comparing the shear strength ratios among the RLC and the other groups, the values for the RLC were generally lower. This indicates that the addition of MSWI-BA, with or without the extra 1 % lime, significantly elevated the shear strength at various stress levels. Table 10 presents the improvement outcomes of 48-h curing period when MSWI-BA (Group 1) or 1 % lime (Group 2) were added, in comparison to the RLC. Since the RLC did not exhibit a significant peak shear strength, only the residual shear strength is compared below. The improvement ratio is defined as the residual shear strength ratio values after 48 h of curing period, divided by the corresponding values of the RLC at each stress level. The average improvement ratio is calculated as the mean value across the three stress levels. According to the average improvement ratios, the addition of MSWI-BA and lime significantly increased the shear strength ratios compared to the ratios of the RLC. Notably, the improvement effect became more pronounced with increasing vertical stresses. According to Table 10, the average improvement ratios ranged from 1.439 to 2.460 across vertical stresses ranging from 85.5 kPa to 259.3 kPa.

Based on the data in Tables 8 and 9, Figs. 6–9 visualized fitting curves and equations with R^2 values. The R^2 values generally indicate good model fitting. However, some values fluctuated within a small range, resulting in poor R^2 values. This was observed, for instance, across all weight ratios of the residual stress ratio in Group 1 with 0 % lime added.

By observing the established curves, in Group 1, the curves of the 48-h curing period generally provide higher values compared to other curing periods, while the curves of the 24-h generally represent the lowest values. For Group 2, the highest values are generally provided by the 72-h fitting curves, while the 24-h fitting curves generally represent the lowest values. The information above provides a suitable approach of upper bound and lower bound shear strength ratio values for the corresponding vertical stress levels, summarized in Tables 11 and 12. The upper and lower bounds are determined based on the equations that relate the input vertical stress values (represented by "x" in kPa) to the corresponding peak or residual shear strength ratio value (represented by "y").

Note that, due to the data limitation of the vertical stress ranging from 85.5 kPa to 259.3 kPa, predictions made outside this vertical stress range may not be applicable. The mixing ratios utilized in this study were constrained to a range between 40 % and 120 %. Additionally, the lime content in the mixtures was either excluded (0 % lime) or included at a minimal level (1 % lime). These

Table 10
Comparing the 48-h curing period improvement ratios on shear strength ratios of Group 1 and 2 to the RLC.

Vertical Stress (kPa)	Mixing Ratio	Group 1: 0 % Lime		Group 2: 1 % Lime	
		Improvement Ratio	Average Improvement Ratio	Improvement Ratio	Average Improvement Ratio
85.5	40 %	1.476	1.439	1.857	1.597
	80 %	1.476		1.572	
	100 %	1.291		1.512	
	120 %	1.512		1.447	
172.4	40 %	2.387	2.240	2.230	2.258
	80 %	2.387		2.409	
	100 %	2.135		2.111	
	120 %	2.052		2.280	
259.3	40 %	2.107	2.318	2.652	2.460
	80 %	2.314		2.555	
	100 %	2.253		2.136	
	120 %	2.596		2.496	

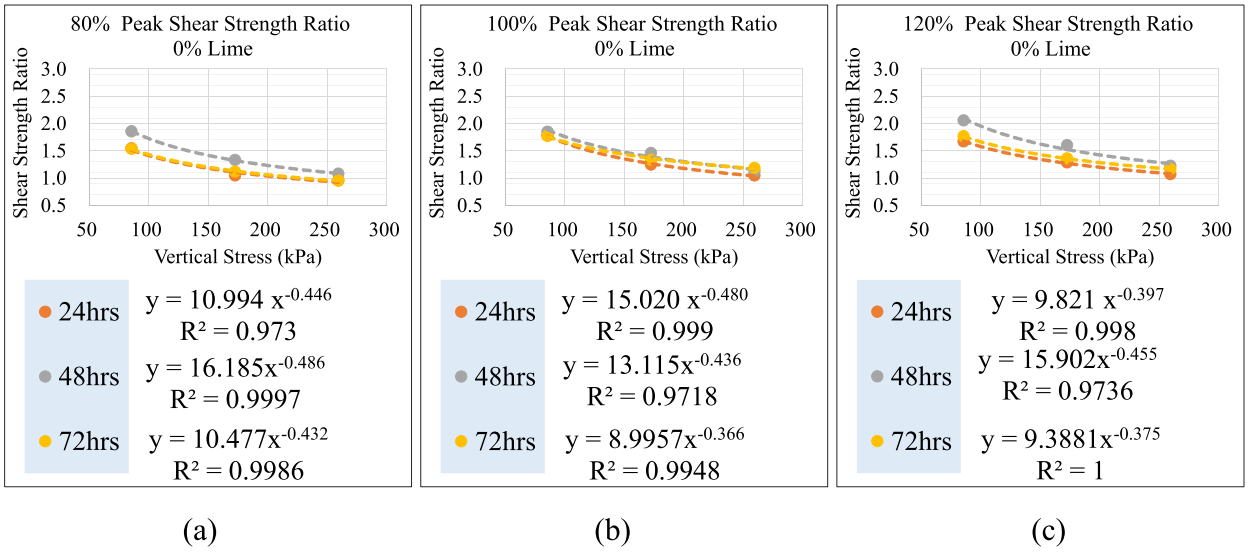

Fig. 6. Plots of peak shear strength ratio versus vertical stress of test Group 1 with of 0 % lime added: (a) 80 % mixing ratio, (b)100 % mixing ratio, and (c) 120 % mixing ratio.

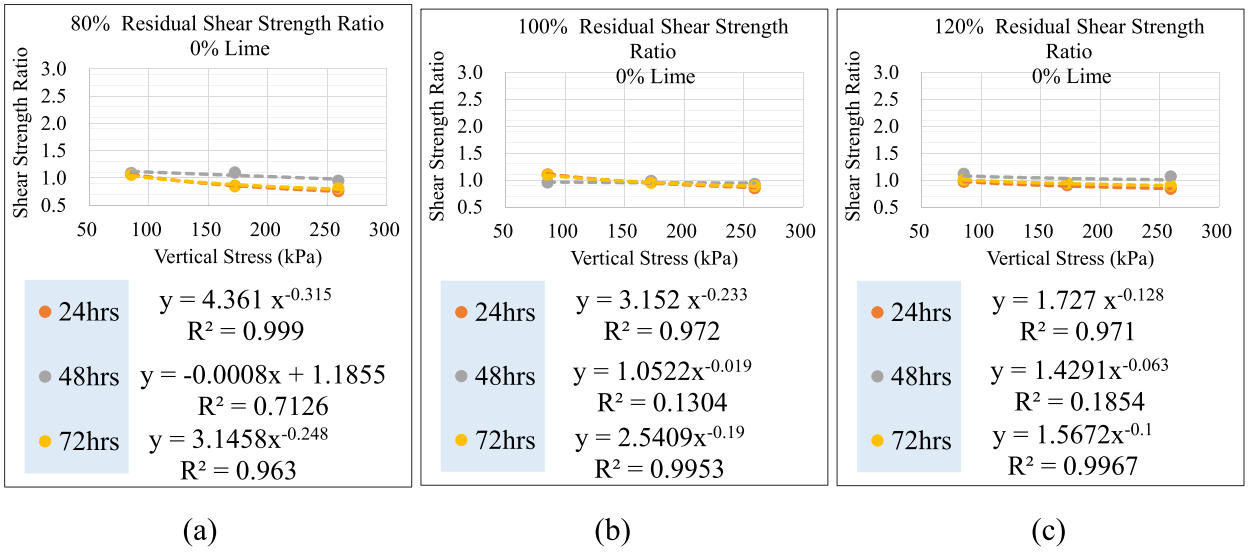

Fig. 7. Plots of residual shear strength ratio versus vertical stress of test Group 1 with of 0 % lime added: (a) 80 % mixing ratio, (b)100 % mixing ratio, and (c) 120 % mixing ratio.

parameters had been strictly adhered to in order to maintain consistency and reliability of the experimental results for future applications.

3.4. Behaviors of cohesion and friction angle

This section aims to establish the strength parameters of the mixtures, including cohesion and friction angle. These parameters are determined using the widely employed Mohr-Coulomb failure criterion model. The goal is to ensure that the designed mixture has the strength and stability required to withstand anticipated loads in geotechnical design applications. For the RLC, based on 2 test sets for each of the 3 stress levels, the cohesion and friction angle values at residual conditions were 40.0 kPa and 14.0°, respectively. Tables 13 and 14, presented below, provide summaries of the cohesion and friction angle values at both peak and residual shear strength conditions for Group 1 and Group 2. Note that, the results of 40 % mixing ratio with a 48-h curing period in Group 1 show no significant peak shear strength development.

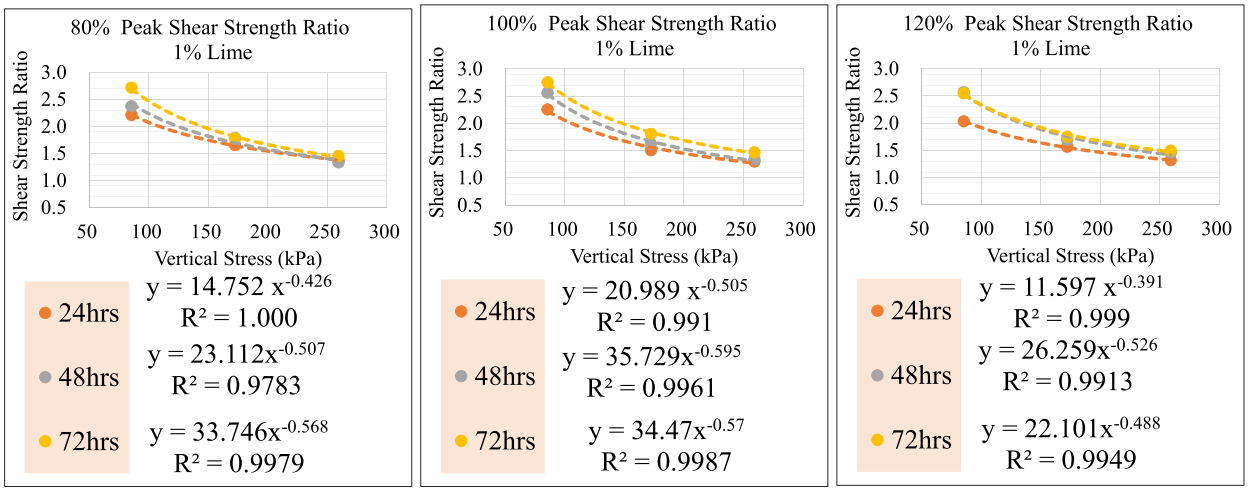

Fig. 8. Plots of peak shear strength ratio versus vertical stress of test Group 2 with of 1 % lime added: (a) 80 % mixing ratio, (b)100 % mixing ratio, and (c) 120 % mixing ratio.

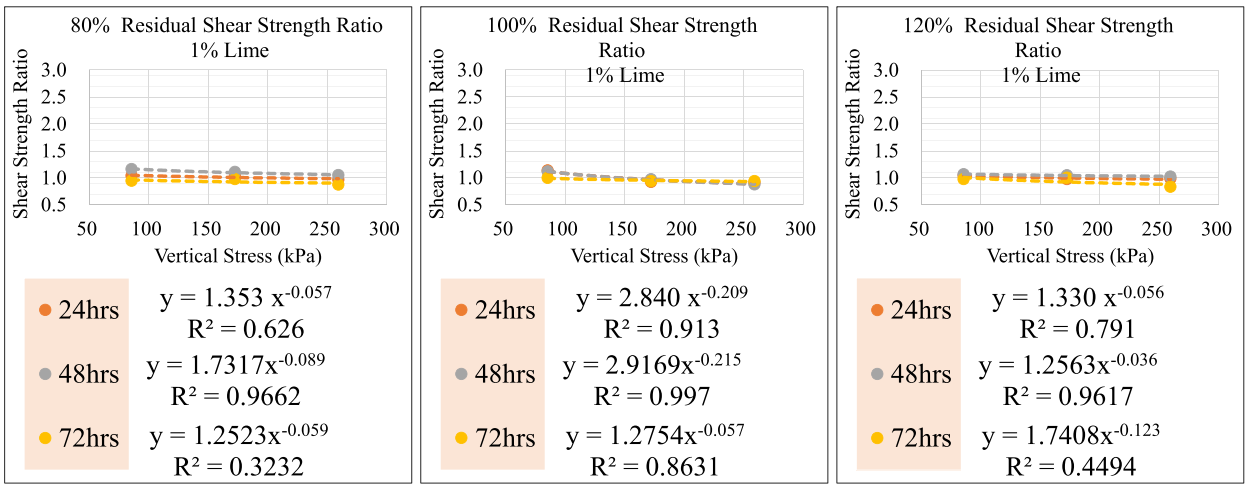

Fig. 9. Plots of residual shear strength ratio versus vertical stress of test Group 2 with of 1 % lime added: (a) 80 % mixing ratio, (b)100 % mixing ratio, and (c) 120 % mixing ratio.

Table 11
The upper and lower bound values of peak and residual shear stress ratios for Group1 (0 % lime added) test program.

Group 1: 0 % Lime		Mixing Ratios		
		80 %	100 %	120 %
Peak Shear Strength Ratio	Upper Bound	$y = 16.185x^{-0.486}$	$y = 13.115x^{-0.436}$	$y = 15.902x^{-0.455}$
	Lower Bound	$y = 10.994x^{-0.446}$	$y = 15.020x^{-0.480}$	$y = 9.821x^{-0.397}$
Residual Shear Strength Ratio	Upper Bound	$y = 1.814x^{-0.109}$	$y = 2.541x^{-0.190}$	$y = 1.429x^{-0.063}$
	Lower Bound	$y = 4.361x^{-0.315}$	$y = 1.052x^{-0.019}$	$y = 1.727x^{-0.128}$

Table 15 provides a statistical summary for the parameters of interests. The statistical parameters include the calculation of mean (μ), standard deviation (σ), and coefficient of variation (COV) for cohesion and friction angle values in both Group 1 and Group 2. While an earlier discussion on the mobilized shear strength and strain unveiled the optimal mixing ratio as 100 %, these parameters in

Table 12
The upper and lower bound values of peak and residual shear stress ratios for Group2 (1 % lime added) test program.

Group 2: 1 % Lime		Mixing Ratios		
		80 %	100 %	120 %
Peak Shear Strength Ratio	Upper Bound	$y = 33.743x^{-0.568}$	$y = 34.470x^{-0.570}$	$y = 22.101x^{-0.488}$
	Lower Bound	$y = 14.752x^{-0.426}$	$y = 20.989x^{-0.505}$	$y = 11.597x^{-0.391}$
Residual Shear Strength Ratio	Upper Bound	$y = 1.732x^{-0.089}$	$y = 1.353x^{-0.057}$	$y = 1.256x^{-0.036}$
	Lower Bound	$y = 1.252x^{-0.059}$	$y = 1.275x^{-0.057}$	$y = 1.741x^{-0.123}$

Table 13
The cohesion and friction angle values of peak and residual shear strength conditions for Group1 (0 % lime added) test program.

Group 1: 0 % Lime		Peak Shear Strength Condition			Residual Shear Strength Condition		
Mixing Ratio	Parameters	24 h	48 h	72 h	24 h	48 h	72 h
40 %	Cohesion (kPa)	–	–	–	–	31.4	–
	Friction Angle (degree)	–	–	–	–	36.3	–
80 %	Cohesion (kPa)	71.9	97.5	75.5	41.4	20.7	37.1
	Friction Angle (degree)	33.7	36.7	33.7	31.1	40.3	32.1
100 %	Cohesion (kPa)	84.1	88.3	75.1	32.3	10.9	26.6
	Friction Angle (degree)	37.9	41.5	42.0	35.7	41.1	38.3
120 %	Cohesion (kPa)	80.1	101.6	79.3	18.9	11.9	14.4
	Friction Angle (degree)	38.7	43.3	41.0	37.7	42.8	40.3

Table 14
The cohesion and friction angle values of peak and residual shear strength conditions for Group2 (1 % lime added) test program.

Group 2: 1 % Lime		Peak Shear Strength Condition			Residual Shear Strength Condition		
Mixing Ratio	Parameters	24 h	48 h	72 h	24 h	48 h	72 h
40 %	Cohesion (kPa)	–	144.4	–	–	37.9	–
	Friction Angle (degree)	–	43.1	–	–	40.9	–
80 %	Cohesion (kPa)	110.6	118.7	140.2	16.0	17.5	13.9
	Friction Angle (degree)	44.0	43.9	42.8	41.9	43.0	40.0
100 %	Cohesion (kPa)	105.5	112.5	139.4	33.6	3.2	6.4
	Friction Angle (degree)	41.8	44.2	44.4	36.4	42.2	42.4
120 %	Cohesion (kPa)	86.0	129.4	134.1	6.1	11.8	11.9
	Friction Angle (degree)	46.3	43.4	44.3	43.8	43.3	41.5

Table 15 are scrutinized at both peak and residual shear strength conditions, considering mixing ratios of 100 % and 120 %. Furthermore, for the purpose of assessing the long-term strength parameters during the facility service life, only the results from 48-h and 72-h fast-curing periods were considered. Table 15 thus provides the recommended cohesion and friction angle values for both peak and residual shear strengths, encompassing variations in mixing ratios (100 % and 120 %) and lime content (0 % or 1 %), with curing periods of 48-h and 72-h.

While considering clayey soils mixed with MSWI-BA and lime, the cohesion and friction angle values are influenced by chemical (pozzolanic reaction) and mechanical (granular behavior) effects. Introduction of 1 % lime notably increased cohesion from 86.1 kPa in Group 1–128.9 kPa in Group 2, while the friction angle saw a smaller rise from 41.9° to 44.1°. This is attributed to a stronger pozzolanic reaction from the added lime, enhancing cementation. Even without lime, MSWI-BA's pozzolanic reaction improved

Table 15
Statistical summary for cohesion and friction angle at peak and residual shear strength conditions for Group1 (0 % lime added) and 2 (1 % lime added) test programs.

	Parameters	Statistical Summary	Peak Shear Strength Condition	Residual Shear Strength Condition
Group 1, 0 % Lime	Cohesion (kPa)	μ	86.1	16.0
		σ	11.7	7.3
		COV	0.14	0.46
	Friction Angle (degree)	μ	41.9	40.6
		σ	1.0	1.9
		COV	0.02	0.05
Group 2, 1 % Lime	Cohesion (kPa)	μ	128.9	8.3
		σ	11.7	4.3
		COV	0.09	0.51
	Friction Angle (degree)	μ	44.1	42.4
		σ	0.4	0.7
		COV	0.01	0.02

cohesion and friction angles at various mixing ratios. For instance, comparing the RLC to Group 1 (48-h curing, 120 % mixing ratio) at peak strength, cohesion rose from 49.2 kPa to 101.6 kPa, and friction angle from 17.7° to 43.3°.

Besides the pozzolanic reaction, the granular behavior can significantly impact the mixture's strength characteristics during large strain conditions. Upon reaching the peak shear strength, increasing the shear force on the specimen led to the gradual development of a shearing surface, resulting in the disruption of cementation bonds along the shear plane. This process diminished the cohesion values to a minimal level. The addition of MSWI-BA caused alterations in the grain size distribution, thereby amplifying the granular effect in the mixture. Under large strain conditions, the shearing mechanism manifested as granular collision behavior within the slipping plane during the high strain phase. This subsequent resistance of the mixture to shear forces was predominantly influenced by the granular behavior arising from the interaction between the mixture and MSWI-BA.

Table 16 summarizes the results of cohesion and friction angle values from this study and others. In comparison with other studies, the current study reports cohesion values ranging from 8.3 kPa to 128.9 kPa for MSWI-BA mixture samples without and with 1 % lime addition, respectively. These values are considerably higher than those reported in other references, such as the 7.7–34.4 kPa range found by Muhunthan et al. (2004) [77] for MSWI-FA, and the 1.3–31.3 kPa range reported by Juarez et al. (2023) [19] for MSW. In the study by Wei et al. (2019) [78], with MSWI-FA combined with shale ash mixed with silty sand, the cohesion values range from 53.3 to 77.44 kPa. The friction angles observed in this study range from 40.6° to 44.1°, which are within the higher end of the ranges reported in other studies. For example, Weng et al. (2010) [79] reported friction angles between 34.8° and 51.1° for dry conditions and 26.0°–37.2° for saturated conditions, while Wei et al. (2019) [78] recorded values between 24.14° and 35.61°. This improvement is likely due to better interlocking between particles and the strengthened behavior of the materials, particularly the granular components. The slight difference between the peak and residual friction angles suggests that the MSWI-BA, with its granular nature, contributes to this stability. The addition of 1 % lime increases the peak friction angle, indicating a noticeable break in bonding at peak conditions, further enhancing the material's shear strength during the peak state.

3.5. Behaviors of dilatancy

By adopting the dilatancy behavior of sand described by Bolton (1986) [25], Equation (1) is utilized in this study for mixture dilatancy analysis. This equation considers the apparent peak friction angle (ϕ_{ps}), apparent residual friction angle (ϕ_{rs}), dilation angle (ψ_d), and parameter of dilatancy coefficient (α) to describe the relationship between dilatancy with various stress conditions. The corresponding parameters in Equation (1) are: τ_p, the maximum shear strength of the mixture at the peak state; σ_v, the vertical stress applied to specimen; τ_r, the residual shear strength at large strains; ε_{vp}, the vertical strain at τ_p; and ε_{hp}, the horizontal shear strain at τ_p. For the sign convention, the positive value of ε_{vp} indicates the dilative behavior.

$$\phi_{ps} = \phi_{rs} + \alpha \times \psi_d \tag{1}$$

where, $\phi_{ps} = tan^{-1}\left(\tau_p/\sigma_v\right)$.

$$\phi_{rs} = tan^{-1}\left(\tau_r/\sigma_v\right)$$

$$\psi_d = tan^{-1}\left(\varepsilon_{vp}/\varepsilon_{hp}\right)$$

As shown in Figs. 10 and 11, in both Group 1 and Group 2, the values of ϕ_{ps} displayed a decreasing trend with increasing vertical stress level. Specimens in Group 2 consistently exhibited higher values of ϕ_{ps} compared to Group 1. Similarly, for both Group 1 and Group 2, the values of ϕ_{rs} showed a slight decrease with increased vertical stress level. However, this decreased tendency of ϕ_{rs} was minimal compared to ϕ_{ps}, and the values were consistently estimated within the range of 40–50°. When comparing different mixing ratio values, the values of ϕ_{ps} show an increasing tendency with increased mixing ratios. For values of ϕ_{rs}, the correlation with mixing ratio values is not obvious. The values of ψ_d decrease with increased vertical stress level in both Group 1 and Group 2. The presence of 1 % lime in Group 2 resulted in higher values of dilation angle compared to Group 1.

Fig. 10(j)–(l) and Fig. 11(j)–(l) present variations in the α values according to various conditions on vertical stress level, mixing ratio, and curing periods. In Group 1, the α values generally increased with the vertical stress level, indicating a positive correlation between the two parameters. However, in Group 2, the α values did not show a strong correlation with different vertical stress levels. Regarding the effect of mixing ratios, the α values in Group 1 were highly influenced by the mixing ratios. For instance, under the condition of 85.5 kPa, 100 % mixing ratio, and a 48-h curing period, the α value was 0.64. Conversely, under the condition of 259.3 kPa with the same mixing ratio and curing period, the α value increased to 0.85. However, in Group 2, the α values did not exhibit a strong correlation with mixing ratios. Turning to the effect of curing periods, in Group 1, the 24-h curing period resulted in higher α values compared to the 48-h and 72-h periods at the same vertical stress level. In Group 2, on the other hand, the α values were the highest under the 72-h curing period compared to the other curing periods.

Unlike the friction angles defined in the Mohr-Coulomb failure criterion, the ϕ_{ps} and ϕ_{rs} were defined specifically at the stress conditions corresponding to the peak and residual shear strength conditions. The calculation of these angles considered the combined effect of the pozzolanic reaction and granular effect. The ϕ_{ps} represented the shear strength condition at the peak state, involving both

Table 16
Comparisons of cohesion and friction angle values.

Sources	Testing approach	Choesion (kPa)	Friection angle (degree)	Marterial descriptions
This study	Direct shear test	86.1/16.0* 128.9/8.3**	41.9/40.6* 44.1/42.4**	MSWI-BA-RLC, and option of 1 % lime added
Weng et al. (2010) [79]	Direct shear test	–	34.8–51.1 (dry) 26.0–37.2 (saturated)	MSWI-BA
Muhunthan et al. (2004) [77]	Direct shear test	7.7–34.4	20.8–50.7	MSWI-FA
Wei et al. (2019) [78]	Triaxial test	53.3–77.44	24.14–35.61	MSWI-FA and shale ash mixed with silty sand
Dehdari et al. (2021) [20]	Direct shear test	0	31.4° (consolidated-drained) and 38.6° (consolidated-undrained)	MSW
Juarez et al. (2023) [19]	Direct shear test	1.3–31.3	3.2–42.9	MSW

*: Group 1 with 0 % lime, in peak/residual shear strength conditions.
**: Group 2 with 1 % lime, in peak/residual shear strength conditions.

the shearing of the cementation bounding of pozzolanic reaction within the RLC, and the mobilization of granular effect strength provided from the MSWI-BA. Across all mixing ratios, the ϕ_{ps} values of Group 2 at different stress levels are generally higher than those of Group 1. On the other hand, with the cementation bounding along the slipping plane gradually fractured, the ϕ_{rs} reflected the shear strength of the sheared fragments of the cemented RLC and the granular effect strength provided from the MSWI-BA materials, particularly at large strains. Upon examining Figs. 10 and 11, it can be noted that the ϕ_{rs} values for both Group 1 and Group 2 remain within a comparable range.

Table 17 summarizes the statistical parameters of α values by considering the absence of lime in Group 1 and the addition of 1 % lime in Group 2. Applying a similar approach as demonstrated in Table 15, these statistical values were derived from mixing ratios of 100 % and 120 %, alongside curing periods of 48-h and 72-h Table 18 lists comparisons of the α values with other references. This study employs MSWI-BA, a material analogous to granular substances, mixed with clayey soil, which is expected to exhibit minimal dilation behavior. In comparison, other studies have examined pure granular materials, such as sands and glass beads, known for their pronounced dilative behavior. The α values obtained in this study ranged from 0.61 to 0.71, which aligned with the ranges reported for other studies. Specifically, the highest α value recorded in this study was 1.17, which is comparable to the maximum value of 1.02 reported by Dai et al. (2016) [23] for glass beads. Additionally, the minimum α value of 0.32 in this study exceeded the lower bound of 0.19 reported by Deng et al. (2021) [22] for sands and glass beads. These findings indicated that the inclusion of MSWI-BA and lime in the mixture results in a noticeable dilative behavior, thereby enhancing the material's strength.

3.6. Discussions on the chemical and mechanical effects

The integration of MSWI-BA and lime into RLC presented a promising approach for soil stabilization, offering significant benefits through both chemical and mechanical enhancements. This study evaluated the effects of MSWI-BA and lime on the strength characteristics of the clay, focusing on the pozzolanic reactions that improve cohesion and friction, as well as the granular behavior that enhanced shear strength and dilatancy.

The pozzolanic reaction resulting from the addition of MSWI-BA and lime is primarily driven by the *CaO* content present in these materials. The *CaO*, upon reacting with water absorbed from the clay, forms calcium hydroxide, which further reacts with the silica and alumina present in the soil to create cementitious compounds. This study employed a fast-curing approach over 24, 48, and 72 h in a controlled environment, which provided optimal conditions for pozzolanic reactions to occur, thereby enhancing inter-particle bonding within the mixture. In this study, various mixing ratios of MSWI-BA-RLC mixture—specifically 40 %, 80 %, 100 %, and 120%—were introduced, both with and without the addition of 1 % lime. These mixtures resulted in a significant increase in cohesion at peak shear strength. However, once the peak shear strength was reached, the structural integrity of the mixture was compromised, resulting in a significant decrease in cohesion. In the residual condition, the mixture's ability to maintain cohesion diminished, ultimately decreasing to negligible levels, reflecting the breakdown of the internal structure following peak loading.

The mechanical effects observed in the mixture were primarily attributed to the granular nature of the MSWI-BA. As the mixing ratio of MSWI-BA in the RLC increased, there was a substantial enhancement in the friction angle values of the mixture. This increased friction angle was sustained at a high level across both peak and residual shear strength conditions, indicating a consistent improvement in shear resistance. Additionally, the mixture inherited the dilative behavior characteristic of granular materials like MSWI-BA. This was evident from the values of the dilatancy coefficient, which demonstrated the mixture's tendency to expand in volume under shear stress applied. Notably, the dilative behavior exhibited by the mixture approached the upper bound values of the dilatancy coefficient typically observed in granular materials, such as sands and glass beads, further contributing to the overall stability and strength of the mixture.

By combining the effects of pozzolanic reactions and the granular nature of MSWI-BA, this approach demonstrated a significant overall improvement in both peak and residual shear strength of the mixture. The synergy between these two mechanisms greatly enhanced the peak and residual strength values, as well as the corresponding shear strength ratios. When compared to the RLC, this

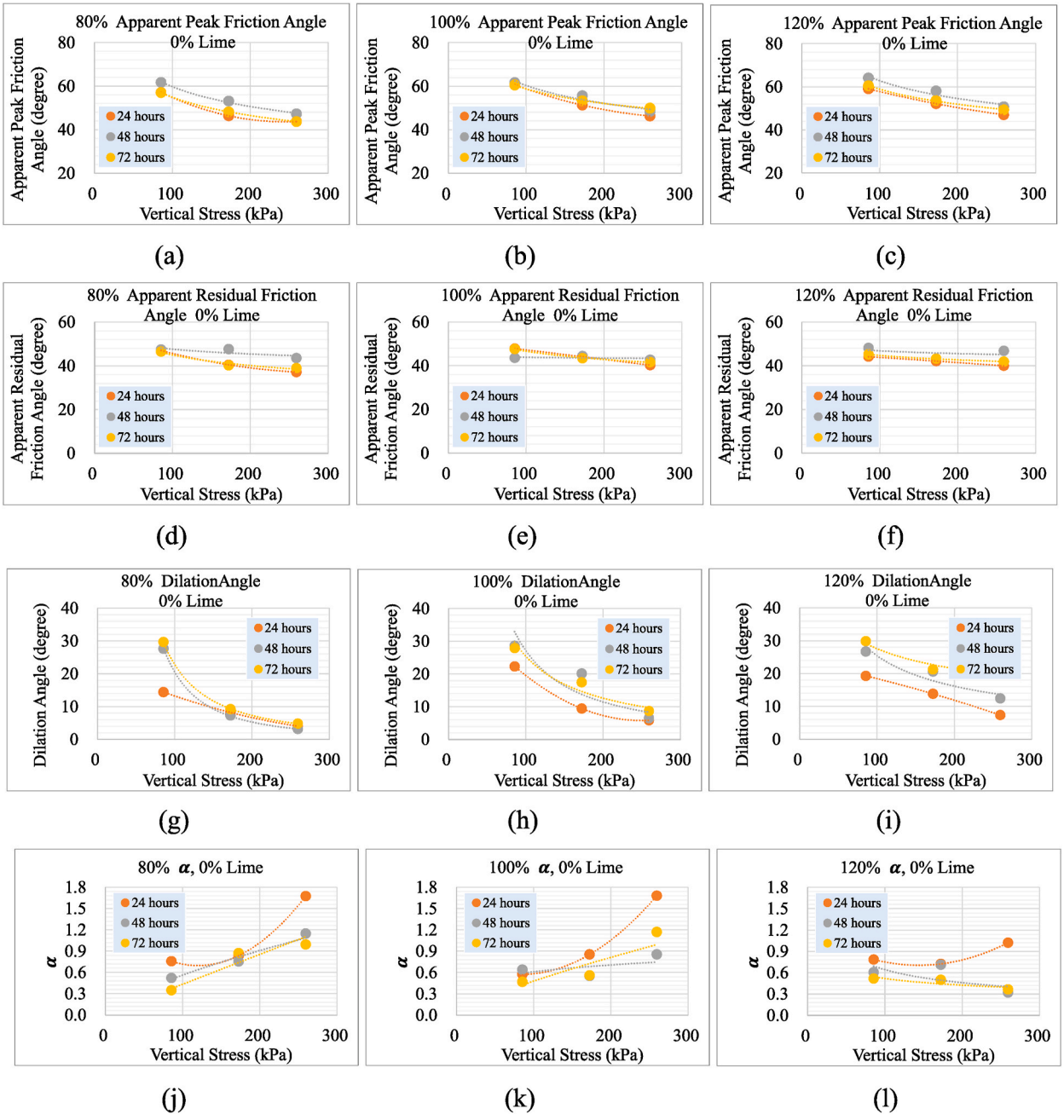

Fig. 10. Plots of dilatancy analysis versus various mixing ratio values and curing periods for Group 1 (0 % lime added) test programs.

method resulted in a substantial increase in shear strength, highlighting the effectiveness of incorporating MSWI-BA and lime in the stabilization process.

By integrating all the aforementioned benefits, the following outlines the potential advantages of using MSWI-BA in civil engineering design and construction.

1 Reusing local soils and cost saving: When local soil is clayey, it typically requires removal and replacement with more suitable materials to meet construction standards. However, by mixing local clayey soils with MSWI-BA, these soils can be effectively reused, eliminating the need for costly material replacement and promoting more sustainable construction practices.
2 Recycling waste materials: Recycling MSWI-BA for civil engineering applications, such as roadway projects, effectively eliminates the need for landfill disposal or long-term storage of this material. This practice reduces redundant space usage and mitigates the

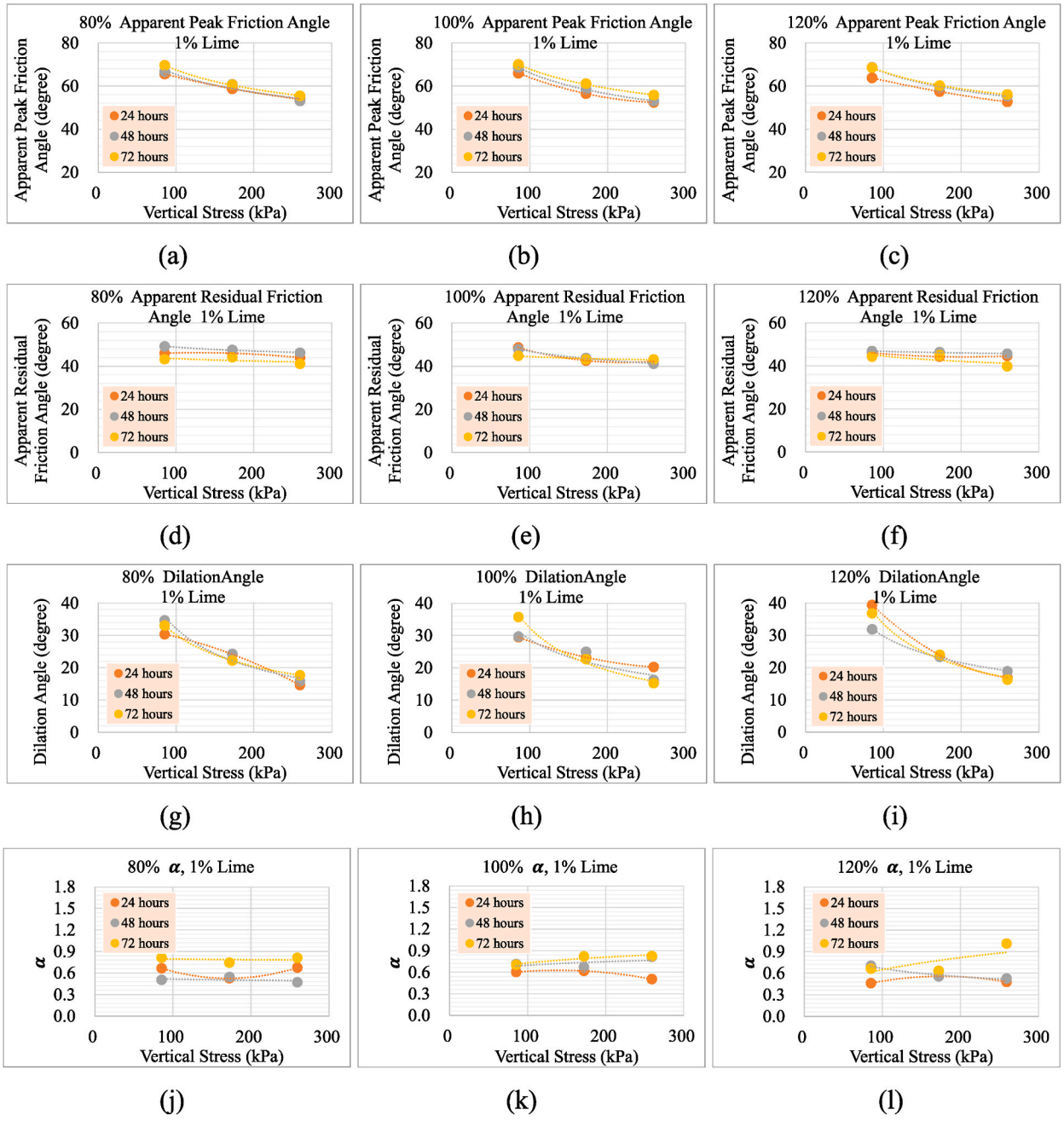

Fig. 11. Plots of dilatancy analysis versus various mixing ratio values and curing periods for Group 2 (1 % lime added) test programs.

Table 17
Statistical summary for dilatancy coefficient (α) values for Group1 (0 % lime added) and 2 (1 % lime added) test programs.

α Statistics	Group 1: 0 % Lime	Group 2: 1 % Lime
Maximum Value	1.17	1.01
Minimum Value	0.32	0.52
μ	0.61	0.72
σ	0.23	0.13
COV	0.38	0.18

Table 18
Comparisons of dilatancy coefficient (α) values.

Sources	Testing approach	Dilatancy coefficient (α) value	Marterial descriptions
This study	Direct shear test	Mean values of 0.61–0.71 with statistic descriptions	MSWI-BA-RLC, and option of 1 % lime added
Bolton (1986) [25]	Plane-strain tests	0.8	Sands
Frydman et al. (2007) [80]	Triaxial test	0.4	Sands
Dai et al. (2016) [23]	Direct shear test	0.59–1.02	Glass beads
Deng et al. (2021) [22]	Triaxial test	0.19–0.63	Sands and glass beads

potential environmental contamination associated with storing or landfilling waste materials, thereby contributing to more sustainable and environmentally responsible waste management practices.

3 Carbon footprint reduction: The incorporation of local materials and MSWI-BA in civil engineering projects substantially reduces the carbon footprint associated with the production of virgin materials. Additionally, this approach minimizes the transportation and construction activities that are traditionally significant contributors to CO_2 emissions. Consequently, the overall environmental impact is mitigated, aligning with the goals of sustainable construction and reducing the generation of greenhouse gases.

4 MSWI-BA-RLC Mixture advantages: All the benefits discussed above are rooted in the proven advantages of the mixture examined in this study, which concludes the substantial improvements in strength characteristics achieved by reusing local clayey soils in combination with recycled MSWI-BA. These enhancements are directly linked to the effective incorporation of MSWI-BA, which transforms the local clay into a stronger and more workable material, thereby enhancing its suitability for a wide range of civil engineering applications.

4. Conclusions

MSWI-BA is increasingly incorporated into civil engineering projects, particularly in soil stabilization and road construction, as a sustainable alternative to traditional materials. By repurposing MSWI-BA, which is often a byproduct of waste management processes, the construction industry significantly reduced the reliance on virgin materials, thereby conserving natural resources and minimizing the environmental impact associated with their extraction and processing. This approach also supports reusing locally available waste materials, effectively turning waste into a valuable resource while diverting it from landfills and mitigating environmental degradation. Additionally, the use of MSWI-BA in construction contributes to a reduction in the carbon footprint, as it decreased the need for energy-intensive production processes associated with conventional materials, and reduced greenhouse gas emissions related to transportation and material production. This study specifically investigated the potential of MSWI-BA in enhancing the mechanical and chemical properties of RLC, a material commonly found in many regions. Through 153 direct shear tests conducted on MSWI-BA-RLC mixtures in this study, the results identified optimal mixing ratios that significantly improved key engineering parameters such as shear strength, cohesion, friction angle, and dilatancy, making the material more suitable for various civil engineering applications. These findings provided valuable data that could guide engineers and researchers in the practical application of MSWI-BA, promoting its use in sustainable civil design and construction projects. Ultimately, this contribution encourages the development of resilient and environmentally responsible infrastructure that met the demands of modern construction while reducing its sustainable footprint.

The following are the important findings in this study.

1. This study aimed to examine the effects of MSWI-BA-RLC mixture by evaluating various factors, including vertical stress, mixing ratio, curing period, and the addition of lime. Vertical stress levels of 86.0 kPa, 129.4 kPa, and 134.1 kPa were selected to simulate low, intermediate, and high stress conditions. Mixing ratios of 40 %, 80 %, 100 %, and 120 % were used to represent potential applications of recycled MSWI-BA while utilizing local soil. A three-way ANOVA analysis was conducted to assess the statistical significance of mixing ratio, curing period, and vertical stress on the average peak and residual shear strength. The analysis revealed that all three factors had a significant effect on the shear strength results in both Group 1 and Group 2, with p-values less than 0.05.
2. The 100 % mixing ratio of MSWI-BA exhibited optimal performance, delivering the optimum peak and residual shear strengths and the most pronounced dilative behavior, both with and without the addition of 1 % lime. This ratio effectively balanced the mechanical and chemical properties, making it the most suitable for enhancing shear strength and dilative characteristics in sustainable design and construction applications.
3. By adding MSWI-BA, with or without 1 % lime, significantly improved the shear strength ratios compared to the RLC, with the average improvement ratios ranging from 1.439 to 2.460 across vertical stresses between 85.5 kPa and 259.3 kPa. The shear strength ratios increased with higher mixing ratios, and the addition of lime further enhanced these ratios.
4. This study established upper-bound and lower-bound relationships between peak and residual strength ratios and vertical stresses, across various mixing ratios. The results are presented in Table 11 for Group 1 with no lime added, and in Table 12 for Group 2 with 1 % lime added.
5. The resulting ranges of cohesion values (8.3–128.9 kPa) and friction angles (40.6°–44.1°) in this study were higher than or within the upper range of those reported in similar research for pure MSWI-BA, MSWI-FA, or MSWI-BA mixtures.
6. The mixing of MSWI-BA and 1 % lime with RLC significantly improved the cohesion and friction angle of the clayey soil. Specifically, the cohesion increased from 40.0 kPa in the RLC to as high as 128.9 kPa with WSIM-BA and addition of 1 % lime, while the

friction angle rose from 14.0° to up to 44.1°. This enhancement is attributed to the pozzolanic reactions and granular behavior introduced by MSWI-BA and lime, which strengthen the material's internal structure.

7. The study utilized Bolton's (1986) [25] dilatancy behavior model to analyze the mixture's dilatancy, focusing on parameters such as peak and residual friction angles, dilation angle, and dilatancy coefficient (α). The α values in this study ranged from 0.61 to 0.71, which are comparable to values reported in other studies on granular materials, such as sands and glass beads. These findings indicate that the inclusion of MSWI-BA and lime in the mixture contributes to noticeable dilative behavior and enhances material strength, similar to or better than those observed in other studies on pure granular materials.
8. The integration of MSWI-BA and lime into RLC proved to be an effective method for soil stabilization, offering significant improvements in strength characteristics through both chemical and mechanical enhancements. The pozzolanic reactions, driven by the *CaO* content in MSWI-BA and lime, significantly increased cohesion and friction angles, while the granular nature of MSWI-BA enhanced shear strength and dilatancy. The study showed that mixing ratios of 40 %–120 % MSWI-BA, with and without 1 % lime, led to substantial increases in peak and residual shear strength, outperforming the RLC. This method also presents notable benefits in civil engineering, including the reuse of local soils, recycling of waste materials, reduction of carbon footprint, and overall improvement in material strength, making it a sustainable and cost-effective approach for construction projects.

While this study provides valuable insights into the potential of MSWI-BA for enhancing RLC properties, several limitations should be acknowledged. The scope was limited to specific factors like vertical stress, mixing ratio, curing period, and lime addition, and the findings are based on controlled laboratory conditions, which may not fully represent real-world applications. Additionally, the environmental risks associated with MSWI-BA, such as potential leachate production and long-term stability, were not explored. Therefore, while the results are promising, further research is needed to validate these findings in diverse conditions and ensure broader applicability and sustainability.

In light of the findings from this study, which highlighted the potential of using MSWI-BA and lime in soil stabilization with local clayey soils, several avenues for future research emerged. These possibilities were aimed at expanding the understanding and efficacy of using recycled materials in construction, enhancing sustainability and reducing environmental impact.

9. Expansion of research variables: Future studies could explore the impact of varying concentrations and ratios of MSWI-BA and lime, and could also include other recycled materials, such as MSWI-FA or recycled concrete aggregate. Investigating these variables could provide deeper insights into the optimal material compositions for different soil types and environmental conditions. This would enable a more tailored application of soil stabilization techniques across diverse geographic and climatic zones.
10. Long-term durability and performance: There is a significant need for longitudinal studies **to assess the long-term performance of soil stabilization using MSWI-BA and lime.** Research could focus on the durability of the stabilized soil under various environmental stressors such as moisture changes and heavy loading. These studies help to further validate the use of these materials in real-world construction projects and for understanding their lifecycle and maintenance requirements.
11. Advanced modeling and simulation: Employing advanced simulation tools and modeling techniques could provide predictive insights into the behavior of stabilized soils over time. These models could help in understanding how different mixtures perform under dynamic load conditions and could optimize the mix designs before they are implemented in the field. Simulation studies could also explore the environmental impact of using these materials, including their carbon footprint and potential leaching of chemical compounds.

Ethical approval

Not required.

Ethics statement

Not applicable.

Data and code availability statement

The data used to support the findings of this study are available from the corresponding author upon request.

CRediT authorship contribution statement

Chwen-Huan Wang: Writing – original draft, Methodology, Formal analysis, Data curation, Conceptualization. **Li Fang:** Writing – review & editing, Formal analysis. **Dave Ta-Teh Chang:** Validation. **Ching-Jui Hsu:** Data curation. **Yu-Tang Hu:** Data curation.

Declaration of competing interest

The authors declare that they have no known competing financial interests or personal relationships that could have appeared to influence the work reported in this paper.

References

[1] N.C. Onat, M. Kucukvar, Carbon footprint of construction industry: a global review and supply chain analysis, Renew. Sustain. Energy Rev. 124 (2020) 109783, https://doi.org/10.1016/j.rser.2020.109783.

[2] B. Sizirici, Y. Fseha, C.-S. Cho, I. Yildiz, Y.-J. Byon, A review of carbon footprint reduction in construction industry, from design to operation, Materials 14 (2021) 6094, https://doi.org/10.3390/ma14206094.

[3] Q. Gao, B. Liu, J. Sun, C. Liu, Y. Xu, Trade decomposition of CO $_2$ emissions of global construction industries, ECAM 29 (2022) 502–522, https://doi.org/10.1108/ECAM-09-2020-0703.

[4] K. Vázquez-Calle, V. Guillén-Mena, F. Quesada-Molina, Analysis of the embodied energy and CO2 emissions of ready-mixed concrete: a case study in cuenca, Ecuador, Materials 15 (2022) 4896, https://doi.org/10.3390/ma15144896.

[5] J. Hong, G.Q. Shen, Y. Feng, W.S. Lau, C. Mao, Greenhouse gas emissions during the construction phase of a building: a case study in China, J. Clean. Prod. 103 (2015) 249–259, https://doi.org/10.1016/j.jclepro.2014.11.023.

[6] M. Weigert, O. Melnyk, L. Winkler, J. Raab, Carbon emissions of construction processes on urban construction sites, Sustainability 14 (2022) 12947, https://doi.org/10.3390/su141912947.

[7] C. Marieta, A. Guerrero, I. Leon, Municipal solid waste incineration fly ash to produce eco-friendly binders for sustainable building construction, Waste Manag. 120 (2021) 114–124, https://doi.org/10.1016/j.wasman.2020.11.034.

[8] S. Zhang, Z. Ghouleh, Y. Shao, Green concrete made from MSWI residues derived eco-cement and bottom ash aggregates, Construct. Build. Mater. 297 (2021) 123818, https://doi.org/10.1016/j.conbuildmat.2021.123818.

[9] D. Chen, Y. Zhang, Y. Xu, Q. Nie, Z. Yang, W. Sheng, G. Qian, Municipal solid waste incineration residues recycled for typical construction materials—a review, RSC Adv. 12 (2022) 6279–6291, https://doi.org/10.1039/D1RA08050D.

[10] P.R. Yaashikaa, P.S. Kumar, A. Saravanan, S. Varjani, R. Ramamurthy, Bioconversion of municipal solid waste into bio-based products: a review on valorisation and sustainable approach for circular bioeconomy, Sci. Total Environ. 748 (2020) 141312, https://doi.org/10.1016/j.scitotenv.2020.141312.

[11] T.A. Kurniawan, W. Lo, D. Singh, M.H.D. Othman, R. Avtar, G.H. Hwang, A.B. Albadarin, A.O. Kern, S. Shirazian, A societal transition of MSW management in Xiamen (China) toward a circular economy through integrated waste recycling and technological digitization, Environ. Pollut. 277 (2021) 116741, https://doi.org/10.1016/j.envpol.2021.116741.

[12] P. Devahi, D. Rathod, K. Muthukkumaran, Building material synthesization using municipal solid waste incineration ash: a state-of-the-art review, Environmental Technology Reviews 11 (2022) 33–48, https://doi.org/10.1080/21622515.2021.2024890.

[13] J. Bawab, J. Khatib, S. Kenai, M. Sonebi, A review on cementitious materials including municipal solid waste incineration bottom ash (MSWI-BA) as aggregates, Buildings 11 (2021) 179, https://doi.org/10.3390/buildings11050179.

[14] S. Kumar, D. Singh, Municipal solid waste incineration bottom ash: a competent raw material with new possibilities, Innov. Infrastruct. Solut. 6 (2021) 201, https://doi.org/10.1007/s41062-021-00567-0.

[15] Y. Zhang, L. Wang, L. Chen, B. Ma, Y. Zhang, W. Ni, D.C.W. Tsang, Treatment of municipal solid waste incineration fly ash: state-of-the-art technologies and future perspectives, J. Hazard Mater. 411 (2021) 125132, https://doi.org/10.1016/j.jhazmat.2021.125132.

[16] D. Zekkos, M. Kabalan, S.M. Syal, M. Hambright, A. Sahadewa, Geotechnical characterization of a municipal solid waste incineration ash from a Michigan monofill, Waste Manag. 33 (2013) 1442–1450, https://doi.org/10.1016/j.wasman.2013.02.009.

[17] N.H. Le, N.E. Abriak, C. Binetruy, M. Benzerzour, S.-T. Nguyen, Mechanical behavior of municipal solid waste incinerator bottom ash: results from triaxial tests, Waste Manag. 65 (2017) 37–46, https://doi.org/10.1016/j.wasman.2017.03.045.

[18] Y. Huang, J. Chen, S. Shi, B. Li, J. Mo, Q. Tang, Mechanical properties of municipal solid waste incinerator (MSWI) bottom ash as alternatives of subgrade materials, Adv. Civ. Eng. 2020 (2020) 1–11, https://doi.org/10.1155/2020/9254516.

[19] M. Juarez, G. Mondelli, H. Giacheti, Shear strength of municipal solid waste rejected from material recovery facilities in the city of São Paulo, Brazil, S&R 46 (2023) e2023013022, https://doi.org/10.28927/SR.2023.013022.

[20] V. Dehdari, M. Ajdari, A. Rostami, Experimental Study on Shear Strength Parameters of Municipal Solid Waste Employing a Large Direct Shear Apparatus, vol. 17, Geomechanics and Geoengineering, 2022, pp. 1184–1199, https://doi.org/10.1080/17486025.2021.1928763.

[21] K.A. Alshibli, M.B. Cil, Influence of particle morphology on the friction and dilatancy of sand, J. Geotech. Geoenviron. Eng. 144 (2018) 04017118, https://doi.org/10.1061/(ASCE)GT.1943-5606.0001841.

[22] Y. Deng, Y. Yilmaz, A. Gokce, C.S. Chang, Influence of particle size on the drained shear behavior of a dense fluvial sand, Acta Geotech 16 (2021) 2071–2088, https://doi.org/10.1007/s11440-021-01143-7.

[23] B.B. Dai, J. Yang, C.Y. Zhou, Observed effects of interparticle friction and particle size on shear behavior of granular materials, Int. J. GeoMech. 16 (2016) 04015011, https://doi.org/10.1061/(ASCE)GM.1943-5622.0000520.

[24] P.W. Rowe, The stress-dilatancy relation for static equilibrium of an assembly of particles in contact, Proc. Roy. Soc. Lond. Math. Phys. Sci. 269 (1962) 500–527.

[25] M.D. Bolton, The strength and dilatancy of sands, Geotechnique 36 (1986) 65–78, https://doi.org/10.1680/geot.1986.36.1.65.

[26] J. Chu, S. Kim, E. Oh, B. Balasubramaniam, D. Bergado, An experimental and theoretical study on the dilatancy of sand and clays, in: Centre for Continuing Education, University of Auckland/New Zealand Geotechnical Society, 2004. https://research-repository.griffith.edu.au/handle/10072/2205. (Accessed 14 June 2023).

[27] Y.H. Wang, S.C. Leung, Characterization of cemented sand by experimental and numerical investigations, J. Geotech. Geoenviron. Eng. 134 (2008) 992–1004, https://doi.org/10.1061/(ASCE)1090-0241(2008)134:7(992.

[28] W.-T. Kuo, Z.-C. Gao, Engineering properties of controlled low-strength materials containing bottom ash of municipal solid waste incinerator and water filter silt, Appl. Sci. 8 (2018) 1377, https://doi.org/10.3390/app8081377.

[29] Z. Tang, W. Li, V.W.Y. Tam, C. Xue, Advanced progress in recycling municipal and construction solid wastes for manufacturing sustainable construction materials, Resour. Conserv. Recycl. X 6 (2020) 100036, https://doi.org/10.1016/j.rcrx.2020.100036.

[30] C.J. Lynn, G.S. Ghataora, R.K. Dhir Obe, Municipal incinerated bottom ash (MIBA) characteristics and potential for use in road pavements, International Journal of Pavement Research and Technology 10 (2017) 185–201, https://doi.org/10.1016/j.ijprt.2016.12.003.

[31] J. An, J. Kim, B.H. Nam, Investigation on impacts of municipal solid waste incineration bottom ash on cement hydration, ACI Mater. J. 114 (2017), https://doi.org/10.14359/51689712.

[32] J. Kim, H. Kim, S. Shin, An evaluation of the physical and chemical stability of dry bottom ash as a concrete light weight aggregate, Materials 14 (2021) 5291, https://doi.org/10.3390/ma14185291.

[33] C.J. Lynn, R.K. Dhir Obe, G.S. Ghataora, Municipal incinerated bottom ash characteristics and potential for use as aggregate in concrete, Construct. Build. Mater. 127 (2016) 504–517, https://doi.org/10.1016/j.conbuildmat.2016.09.132.

[34] J. An, B. Golestani, B.H. Nam, J.L. Lee, Sustainable utilization of MSWI bottom ash as road construction materials, Part I: physical and mechanical evaluation, in: Airfield and Highway Pavements 2015, American Society of Civil Engineers, Miami, Florida, 2015, pp. 225–235, https://doi.org/10.1061/9780784479216.021.

[35] V. Sharma, S. Singh, Modeling for the use of waste materials (Bottom ash and fly ash) in soil stabilization, Mater. Today: Proc. 33 (2020) 1610–1614, https://doi.org/10.1016/j.matpr.2020.05.569.

[36] A. Joseph, R. Snellings, P. Van Den Heede, S. Matthys, N. De Belie, The use of municipal solid waste incineration ash in various building materials: a Belgian point of view, Materials 11 (2018) 141, https://doi.org/10.3390/ma11010141.

[37] D. Singh, A. Kumar, Geo-environmental application of municipal solid waste incinerator ash stabilized with cement, J. Rock Mech. Geotech. Eng. 9 (2017) 370–375, https://doi.org/10.1016/j.jrmge.2016.11.008.

[38] Transportation Research Board. State-of-the-Art Report 5: Reactions, Properties, Design, and Construction, 1987, p. 25. https://trid.trb.org/view/283897 (accessed May 22, 2023).

[39] G.N. Eujine, S. Chandrakaran, N. Sankar, Accelerated subgrade stabilization using enzymatic lime technique, J. Mater. Civ. Eng. 29 (2017) 04017085, https://doi.org/10.1061/(ASCE)MT.1943-5533.0001923.
[40] A. Athanasopoulou, Addition of lime and fly ash to improve highway subgrade soils, J. Mater. Civ. Eng. 26 (2014) 773–775, https://doi.org/10.1061/(ASCE)MT.1943-5533.0000856.
[41] Y. Zhang, J.L. Daniels, B. Cetin, I.K. Baucom, Effect of temperature on pH, conductivity, and strength of lime-stabilized soil, J. Mater. Civ. Eng. 32 (2020) 04019380, https://doi.org/10.1061/(ASCE)MT.1943-5533.0003062.
[42] R. Feng, L. Wu, D. Liu, Y. Wang, B. Peng, Lime- and cement-treated sandy lean clay for highway subgrade in China, J. Mater. Civ. Eng. 32 (2020) 04019335, https://doi.org/10.1061/(ASCE)MT.1943-5533.0002984.
[43] A. Mohajerani, J. Bakaric, T. Jeffrey-Bailey, The urban heat island effect, its causes, and mitigation, with reference to the thermal properties of asphalt concrete, J. Environ. Manag. 197 (2017) 522–538, https://doi.org/10.1016/j.jenvman.2017.03.095.
[44] Y. Liu, Y. Wang, D. Li, Estimation and uncertainty analysis on carbon dioxide emissions from construction phase of real highway projects in China, J. Clean. Prod. 144 (2017) 337–346, https://doi.org/10.1016/j.jclepro.2017.01.015.
[45] F. Ma, A. Sha, R. Lin, Y. Huang, C. Wang, Greenhouse gas emissions from asphalt pavement construction: a case study in China, IJERPH 13 (2016) 351, https://doi.org/10.3390/ijerph13030351.
[46] R. Forteza, M. Far, C. Seguí, V. Cerdá, Characterization of bottom ash in municipal solid waste incinerators for its use in road base, Waste Manag. 24 (2004) 899–909, https://doi.org/10.1016/j.wasman.2004.07.004.
[47] J. Li, B. Tang, R. Liu, Z. Xu, P. Xu, Q. Zhou, Y. Wen, C. Zhong, Characteristics of MSWI fly ash and its resource transformation by road engineering: mechanical and environmental considerations, Construct. Build. Mater. 323 (2022) 126575, https://doi.org/10.1016/j.conbuildmat.2022.126575.
[48] H.-L. Luo, S.-H. Chen, D.-F. Lin, X.-R. Cai, Use of incinerator bottom ash in open-graded asphalt concrete, Construct. Build. Mater. 149 (2017) 497–506, https://doi.org/10.1016/j.conbuildmat.2017.05.164.
[49] A. Vaitkus, J. Gražulytė, O. Šernas, V. Vorobjovas, R. Kleizienė, An algorithm for the use of MSWI bottom ash as a building material in road pavement structural layers, Construct. Build. Mater. 212 (2019) 456–466, https://doi.org/10.1016/j.conbuildmat.2019.04.014.
[50] Yanjun Hu, Guojian Li, Yingjie Zhong, Utilization of municipal solid waste incineration bottom ash as road construction materials, in: 2010 International Conference on Mechanic Automation and Control Engineering, IEEE, Wuhan, China, 2010, pp. 1370–1373, https://doi.org/10.1109/MACE.2010.5536261.
[51] S.W. Townsend, C.J. Spreadbury, S.J. Laux, C.C. Ferraro, R. Kari, T.G. Townsend, Blending as a strategy for reusing municipal solid waste incinerator ash in road-base construction, J. Environ. Eng. 146 (2020) 04020106, https://doi.org/10.1061/(ASCE)EE.1943-7870.0001788.
[52] C.J. Spreadbury, M. McVay, S.J. Laux, T.G. Townsend, A field-scale evaluation of municipal solid waste incineration bottom ash as a road base material: considerations for reuse practices, Resour. Conserv. Recycl. 168 (2021) 105264, https://doi.org/10.1016/j.resconrec.2020.105264.
[53] C. Shi, J. Li, S. Sun, H. Han, Research on pavement performance of cement-stabilized municipal solid waste incineration bottom ash base, Materials 15 (2022) 8614, https://doi.org/10.3390/ma15238614.
[54] R.A. Joumblat, Z. Al Basiouni Al Masri, J. Absi, A. ElKordi, Investigation of using municipal solid waste incineration fly ash as alternative aggregates replacement in hot mix asphalt, Road Mater. Pavement Des. 24 (2023) 1290–1309, https://doi.org/10.1080/14680629.2022.2071756.
[55] K. Park, B. Golestani, B.H. Nam, J. Hou, J. Eun, Study on the combined effect of municipal solid waste incineration bottom ash and waste shingle in hot mix asphalt, Materials 17 (2023) 46, https://doi.org/10.3390/ma17010046.
[56] S. Gowda, V. Kunjar, A. Gupta, V.G. Havanagi, G. Kavitha, Municipal incinerated solid waste bottom ash as sustainable construction material in the construction of flexible pavements, J. Mater. Cycles Waste Manag. 25 (2023) 3824–3833, https://doi.org/10.1007/s10163-023-01809-2.
[57] B.T. Kamtchueng, V.L. Onana, W.Y. Fantong, A. Ueda, R.F. Ntouala, M.H. Wongolo, G.B. Ndongo, A.N. Ze, V.K. Kamgang, J.M. Ondoa, Geotechnical, chemical and mineralogical evaluation of lateritic soils in humid tropical area (Mfou, Central-Cameroon): implications for road construction, Geo-Engineering 6 (2015) 1, https://doi.org/10.1186/s40703-014-0001-0.
[58] M. El Gendy, A. Mohamady, T. Nabil, M. Shams, Effect of the presence of soft clay on the structural design of highway sections, Port-Said Engineering Research Journal 23 (2019) 26–33, https://doi.org/10.21608/pserj.2019.49559.
[59] L. Lizárraga-Mendiola, L.D. López-León, G.A. Vázquez-Rodríguez, Municipal solid waste as a substitute for virgin materials in the construction industry: a review, Sustainability 14 (2022) 16343, https://doi.org/10.3390/su142416343.
[60] A. Soni, P.K. Das, A.W. Hashmi, M. Yusuf, H. Kamyab, S. Chelliapan, Challenges and opportunities of utilizing municipal solid waste as alternative building materials for sustainable development goals: a review, Sustainable Chemistry and Pharmacy 27 (2022) 100706, https://doi.org/10.1016/j.scp.2022.100706.
[61] F. Liu, H. Liu, N. Yang, L. Wang, Comparative study of municipal solid waste incinerator fly ash reutilization in China: environmental and economic performances, Resour. Conserv. Recycl. 169 (2021) 105541, https://doi.org/10.1016/j.resconrec.2021.105541.
[62] A. Assi, F. Bilo, A. Zanoletti, J. Ponti, A. Valsesia, R. La Spina, A. Zacco, E. Bontempi, Zero-waste approach in municipal solid waste incineration: reuse of bottom ash to stabilize fly ash, J. Clean. Prod. 245 (2020) 118779, https://doi.org/10.1016/j.jclepro.2019.118779.
[63] N. Baldo, F. Rondinella, F. Daneluz, M. Pasetto, Foamed bitumen mixtures for road construction made with 100% waste materials: a laboratory study, Sustainability 14 (2022) 6056, https://doi.org/10.3390/su14106056.
[64] H. Chu, Q. Wang, W. Zhang, Optimizing ecological ultra-high performance concrete prepared with incineration bottom ash: utilization of Al2O3 micro powder for improved mechanical properties and durability, Construct. Build. Mater. 426 (2024) 136152, https://doi.org/10.1016/j.conbuildmat.2024.136152.
[65] Q. Wang, H. Chu, J. Jiang, B. Zhu, Enhancing mechanical performance and durability of high strength mortar with incineration bottom ash via Al2O3 micro-powder: an experimental study, J. Build. Eng. 89 (2024) 109268, https://doi.org/10.1016/j.jobe.2024.109268.
[66] Q. Wang, H. Chu, W. Shi, J. Jiang, F. Wang, Feasibility of preparing self-compacting mortar via municipal solid waste incineration bottom ash: an experimental study, Archiv.Civ.Mech.Eng 23 (2023) 251, https://doi.org/10.1007/s43452-023-00794-5.
[67] L. Li, T. Zang, H. Xiao, W. Feng, Y. Liu, Experimental study of polypropylene fibre-reinforced clay soil mixed with municipal solid waste incineration bottom ash, European Journal of Environmental and Civil Engineering 27 (2023) 2700–2716, https://doi.org/10.1080/19648189.2020.1795726.
[68] P. Singh, A. Boora, A.K. Gupta, Sub-grade characteristics of clayey soil incorporating municipal solid waste incineration ash and marble dust, JEDT 20 (2022) 712–726, https://doi.org/10.1108/JEDT-08-2020-0347.
[69] P. Singh, A. Boora, A.K. Gupta, Geotechnical characteristics of clayey soil admixed with municipal solid waste incineration ash, cement and polypropylene fiber, Innov. Infrastruct. Solut. 6 (2021) 193, https://doi.org/10.1007/s41062-021-00547-4.
[70] D. Baruah, S. Goel, C. Gupta, A.K. Sahu, Ground improvement using municipal solid waste ash, in: S.K. Shukla, S.V. Barai, A. Mehta (Eds.), Advances in Sustainable Construction Materials and Geotechnical Engineering, Springer Singapore, Singapore, 2020, pp. 271–280, https://doi.org/10.1007/978-981-13-7480-7_25.
[71] B.J.S. Varaprasad, J.R. Joga, S.R. Joga, Reuse of municipal solid waste from incinerated ash in the stabilization of clayey soils, Slovak Journal of Civil Engineering 28 (2020) 1–7, https://doi.org/10.2478/sjce-2020-0024.
[72] Z.-F. Huang, C.-H. Shen, C.-H. Wang, L.-C. O, L. Fang, D.T.-T. Chang, Study on the incinerated recycle aggregates mixture design and effect parameters for clay soil stabilization, Journal of the Chinese Institute of Civil and Hydraulic Engineering 33 (2021) 61–71, https://doi.org/10.6652/JoCICHE.202103_33(1).0007.
[73] X. Sun, Y. Yi, Amending excavated soft marine clay with fine incineration bottom ash as a fill material for construction of transportation infrastructure, Transportation Geotechnics 35 (2022) 100796, https://doi.org/10.1016/j.trgeo.2022.100796.
[74] Z. Zimar, D. Robert, A. Sidiq, A. Zhou, F. Giustozzi, S. Setunge, J. Kodikara, Waste-to-energy ash for treating highly expansive clays in road pavements, J. Clean. Prod. 374 (2022) 133854, https://doi.org/10.1016/j.jclepro.2022.133854.
[75] K. Qiu, G. Zeng, B. Shu, D. Luo, Study on the performance and solidification mechanism of multi-source solid-waste-based soft soil solidification materials, Materials 16 (2023) 4517, https://doi.org/10.3390/ma16134517.
[76] R.L. Terrel, J.A. Epps, E.J. Barenberg, J.K. Mitchell, M.R. Thompson. Soil Stabilization in Pavement Structures-A User's Manual Volume 1: Pavement Design and Construction Considerations, 1979, p. 132. https://trid.trb.org/view/151443 (accessed May 22, 2023).

[77] B. Muhunthan, R. Taha, J. Said, Geotechnical engineering properties of incinerator ash mixes, J. Air Waste Manag. Assoc. 54 (2004) 985–991, https://doi.org/10.1080/10473289.2004.10470959.
[78] H. Wei, Y. Zhang, J. Cui, L. Han, Z. Li, Engineering and environmental evaluation of silty clay modified by waste fly ash and oil shale ash as a road subgrade material, Construct. Build. Mater. 196 (2019) 204–213, https://doi.org/10.1016/j.conbuildmat.2018.11.060.
[79] M.-C. Weng, C.-L. Lin, C.-I. Ho, Mechanical properties of incineration bottom ash: the influence of composite species, Waste Manag. 30 (2010) 1303–1309, https://doi.org/10.1016/j.wasman.2009.11.010.
[80] S. Frydman, M. Talesnick, H. Nawatha, K. Schwartz, Stress-dilation of undisturbed sand samples in drained and undrained triaxial shear, Soils Found. 47 (2007) 27–32, https://doi.org/10.3208/sandf.47.27.